Australian Government
Bureau of Meteorology

The Centre for Australian Weather and Climate Research
A partnership between CSIRO and the Bureau of Meteorology

CSIRO

CAWCR Research Letters

Issue 1, December 2008

P. A. Sandery, T. Leeuwenburg, G. Wang, A. J. Hollis (editors)

www.cawcr.gov.au

ISSN: 1836-5949

Series: Research Letters (The Centre for Australian Weather and Climate Research); Issue 1.

Copyright and Disclaimer

Contents

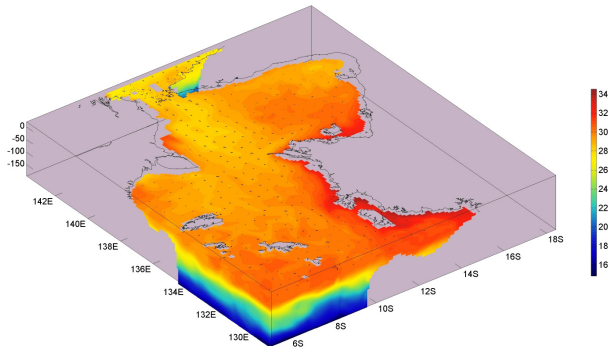

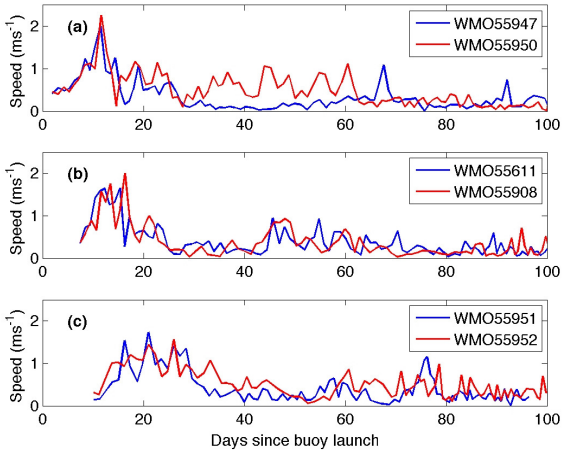

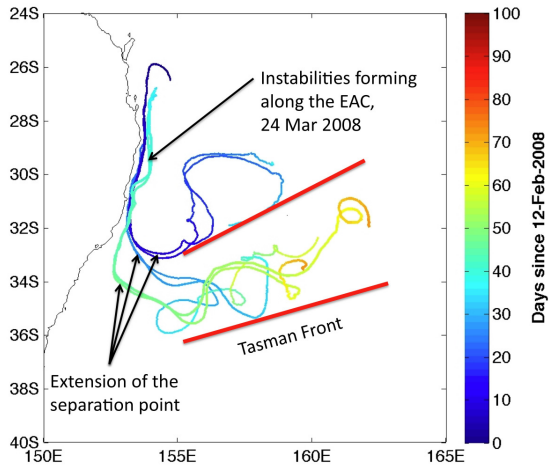

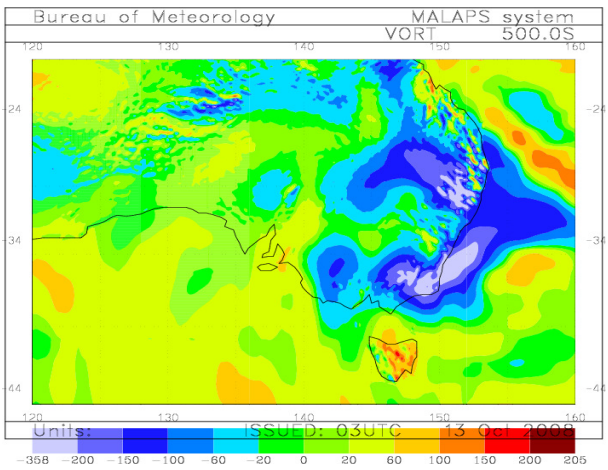

Editors: P. A. Sandery, T. Leeuwenburg, G. Wang, A. J. Hollis
Enquiries: Dr Paul Sandery p.sandery@bom.gov.au
CAWCR Research Letters
The Centre for Australian Weather and Climate Research
Bureau of Meteorology
GPO Box 1298K Melbourne VICTORIA 3001

CAWCR Research Letters is an internal serial online publication aimed at communication of research carried out by CAWCR staff and their colleagues. It follows on from its predecessor *BMRC Research Letters*. Articles in *CAWCR Research Letters* are internally reviewed and 3-5 pages in length. For more information visit the *CAWCR Research Letters* website.

Observed Early Winter Mean Sea Level Pressure Changes over Southern Australia: a comparison of existing datasets

B. Timbal[A] and P. Hope[B]

[AB]Centre for Australian Weather and Climate Research

Bureau of Meteorology

Corresponding author: b.timbal@bom.gov.au

Introduction

Most of southern Australia has seen rainfall declines in the last 50 years (user defined trend maps can be generated on-line on the Bureau of Meteorology web site: http://www.bom.gov.au/silo/products/cli_chg/).

In particular two areas have experienced well documented step changes: the south-west corner of Western Australia (SWWA) in the late 1960s (IOCI, 2002) and the south-eastern part of Australia in the 1990s (Murphy and Timbal, 2007). In Eastern Australia, the area which is most similar to SWWA is the South-Western part of Eastern Australia (SWEA) encompassing western Victoria and southern South Australia. Rainfall variability on daily and interannual time-scales is significantly correlated between the regions, particularly in late autumn and early winter - May-June-July (MJJ) (Hope *et al.*, 2009). MJJ is also a critical period for the long-term rainfall declines.

In both regions, rainfall variability is related closely to local variations of Mean Sea Level Pressure (MSLP) (e.g. Allan and Haylock, 1993; Timbal and Murphy, 2007; Hope *et al.*, 2009). Hope *et al.* (2009) have shown that on inter-annual time-scales, the relationship between the rainfalls in both regions is mostly due to the high correlation of MSLP between both regions. Both SWWA and SWEA, at this time of the year, are centred poleward of the sub-tropical ridge (STR), a belt of high MSLP corresponding to the descending branch of the Hadley Circulation (Peixoto and Oort, 1992).

The significance of the rainfall declines in southern Australia and the importance of the MSLP/rainfall relationship warrant a careful analysis of MSLP trends observed in the surrounding regions with a focus on the MJJ season. This note starts by investigating the long-term MSLP trends using gridded observations and then moves on a careful evaluation of the consistency of the different gridded products (either based on station observations or on model-based reanalyses of the atmosphere) that are available in order to build confidence on more recent MSLP trends.

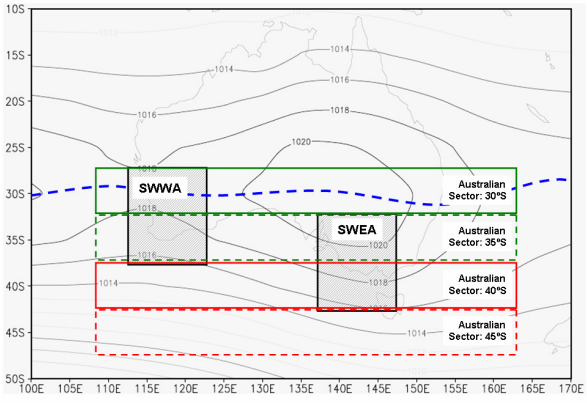

Figure 1. *The long-term 1850 to 2004 mean of MJJ MSLP from the HadSLP2 dataset around the Australian continent. Boxes used to calculate time series are shown: SWWA, SWEA regions as well as Australian sector latitude bands; the position of the mean sub-tropical ridge is shown by a blue dashed line.*

Long Term Perspective

The global HadSLP2 MSLP dataset on a 5º by 5º grid (Allan and Ansell, 2006) spans the years 1850 to 2004, providing the ability to obtain a long-term perspective on MSLP variability and secular changes. The mean climatology of MJJ MSLP in the Australian region exhibits the

location of the STR, with a centre located over eastern Australia, and a permanent long-wave trough affecting Western Australia (Figure 1).

MJJ time series were created for the longitude bands relevant to southern Australian climate (shown in Figure 2, for both an Australian sector from 107.5ºE to 162.5ºE and the entire Southern Hemisphere) and for the two regions having experienced rainfall declines: SWWA from 27.5º to 37.5ºS and 112.5º to 122.5ºE and SWEA from 32.5º to 42.5ºS and 137.5º to 147.5ºE (Figure 3).

The methodology to generate complete gridded data back to 1850 is described in Allan and Ansell (2006). The reader should refer to this paper for a full description of the methodology and the data available to generate the gridded product; only a few details relevant to our study are provided here.

Starting from a broad hemispheric perspective (Figure 2, left), it is clear that overall MSLP has risen during the available historical record in a broad mid-latitude (30°S to 45°S) band; the clarity of this signal grows with latitude. Most of the increase occurred early on in the 20th century. The increase in MSLP over the full record is greatest at higher latitudes; a large part of this difference is due to the increase from the late 1920s to the 1950s. It is also interesting to note that during that period, MSLP started to rise earlier at higher latitude (45ºS) with a greater rate of increase, resulting in large differences in MSLP when MSLP values stabilise from around the 1950s to the 1970s. After the 1970s, MSLP started to rise again. This hemispheric perspective of a southern hemisphere annular signal propagating from higher to lower latitude is contradicted in southern Australia where MSLP increase in SWWA occurred earlier compared to SWEA while SWWA is located closer toward the equator (between 30ºS and 35ºS) than SWEA (between 33ºS and 38ºS).

Indeed, when focusing solely on the Australian sector (from 110ºE to 160ºE; right graph in Figure 2), overall trends are similar, and the difference between the latitudinal bands at 30ºS and 35ºS (which matter most) become indistinguishable. In the Australian sector, there is greater variability (or noise) than for the hemispheric average (note that for both graphs in Figure 2, 21-year running means are plotted). As for the full hemisphere, after the rise in MSLP around the 1940s, pressures at high latitudes remain high, while they drop at other latitudes. After the late 1960s, all latitudes show increasingly high anomalies of MSLP again, although at higher latitudes MSLP has declined sharply since about 1980. The sharp decrease at high latitudes in recent years is even larger at higher latitude 50ºS and 60ºS (not shown) and appears consistent with a Southern Annular Mode (SAM) index positive trend (Marshall, 2003; Gillett *et al.*, 2006). The part of the signal that is spurious due to data issues (Allan and Ansell, 2006 and references therein) is difficult to separate from the climate signal over the long-term historical record, particularly early in the record. The methodology used to generate gridded data is very important.

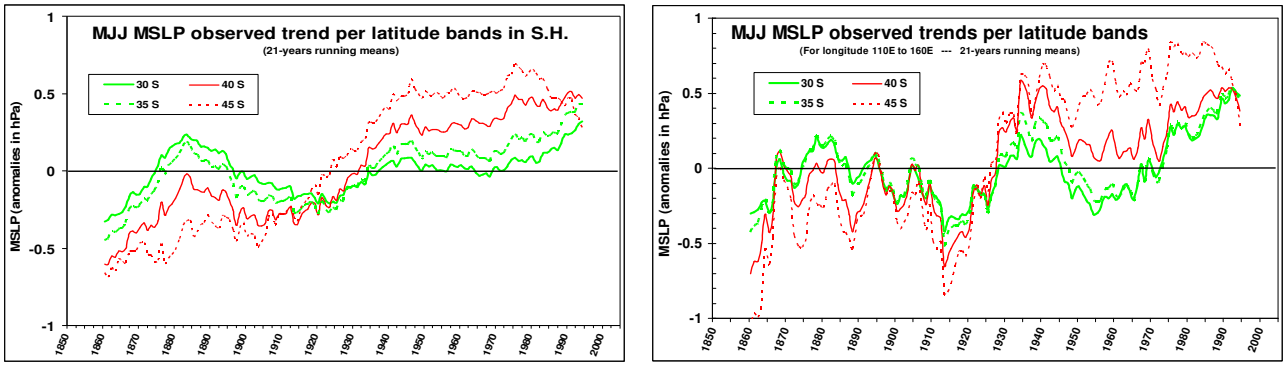

Figure 2. *21-year running mean May, June and July average MSLP anomalies (calculated with respect to the 1850-2004 mean) from the HadSLP2 dataset, over 5º latitude bands (from 30ºS to 45ºS) for the entire Southern Hemisphere (left) and for the Australian sector (110ºE to 160ºE, right).*

Allan and Ansell (2006) used an optimal interpolation method to calculate anomalies (using 34 leading EOFs calculated from existing observations) and smooth them to remove abnormally large grid point spikes. This methodology allows spatio-temporal gaps in the observations to be filled appropriately, but is also likely to smooth out true variability. This will be particularly true in areas of poor data coverage. An analysis of the availability of in-situ observations in the Australian longitudes (110ºE to 160ºE) of the Southern Hemisphere (Figure 3) reveals the lack of constant observations south of 50ºS until the early 1960s with entire decades without a single observation (periods where no whaling ships have reported observations). The wax and wane of available observations is likely to affect the long-term variation of the reconstructed MSLP dataset south of 50ºS (for this reason only time series north of 50ºS were shown).

At the latitudes considered here, the rise in the number of observations in recent decades is also spectacular (note the logarithmic scale on the Y-axis of Figure 3) but starts earlier (around 1955) and there is more data available for the hundred years prior at latitudes between 20ºS to 40ºS. MSLP trends during epochs when the number of observations change markedly might be viewed with caution. During the early period from 1910-1940, where sharp upward trends in MSLP were seen (Fig 2, right), there were of the order of 500 observation points in the first half of the period, rising to over 1000 at 20ºS and 30ºS for about 10 years from the late 1920s before falling again.

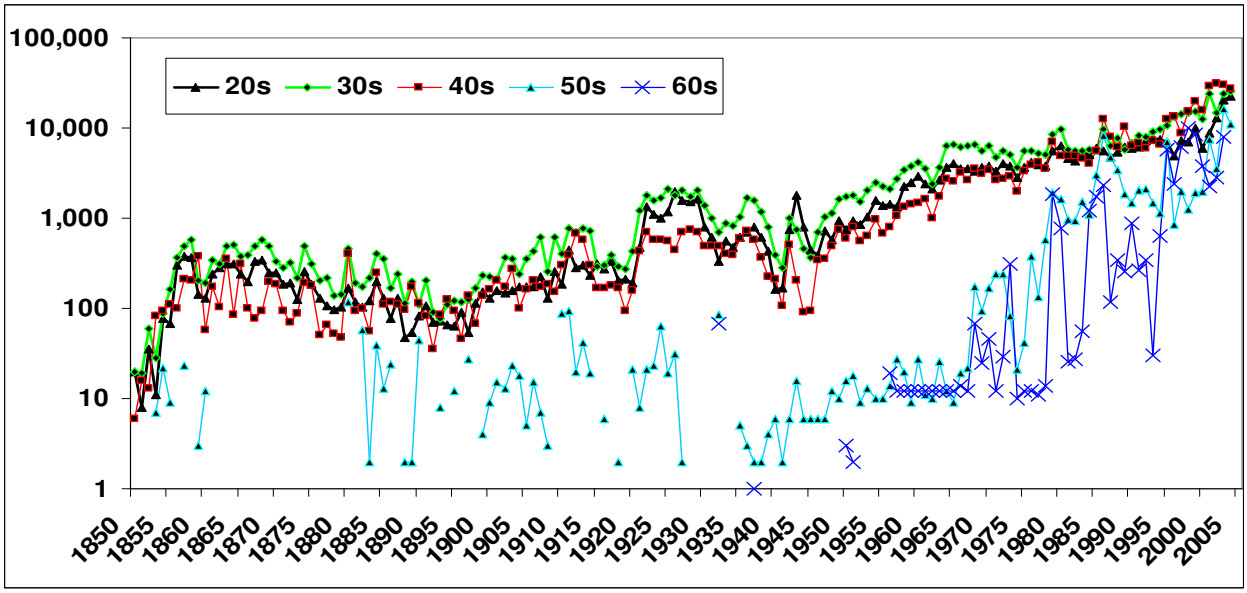

Figure 3. *Number of observations from 1850 to 2004 used to generate the HadSLP2 dataset per 10º latitude bands from 20ºS to 60ºS (e.g. 20s averages 20ºS and 25ºS) in the Australian sector from 110ºE to 160ºE (note the logarithmic scale on the y-axis).*

During this period the trend in MSLP does not falter significantly, suggesting that, although the number of observations varies, the general trend is likely to be accurate. Focusing now on the two small regions of SWWA and SWEA (Figure 4), the MSLP increase throughout the historical record is also quiet noticeable. Consistent with the rainfall decreases in SWWA and SWEA in MJJ, the 11-year running mean of the MSLP anomalies is increasing. However, the MSLP trends in the second half of the 20th century are not the most spectacular compared to earlier periods in the record. Similar or more rapid increases were seen in the early 20th century and in the late 19th

century for both regions. Nevertheless, 11-year running mean MJJ anomalies were in the late 1990s at their highest levels since the beginning of the record for SWEA and at near record values for SWWA. In all cases the last 5 years or so have seen a slight decline from the peak values. MSLP in the two regions is highly correlated as noted by Hope *et al.* (2009) on inter-annual time-scales since 1850 (r=0.80).

The Reanalyses Era

For the second half of the 20th century, additional MSLP climatology can be obtained from re-analyses. Two sets of global reanalyses were analysed: the ERA40 produced by the European Center for Medium-range Weather Forecasting and available from late 1957 to 2002 (Uppala *et al.*, 2005) and the reanalyses jointly produced by the National Centers for Environmental Prediction (NCEP) and for Atmospheric Research (NCAR) (hereafter, NNR) from 1948 to current (Kalnay *et al.*, 1996).

Both datasets provide MSLP with a global coverage on a 2.5° by 2.5° grid and are produced using a frozen global data assimilation system, therefore for the second half of the 20th century it is possible to compare three datasets (shown for MJJ in SWWA and SWEA in Figure 4). The reanalyses used in this study, their availability, quality concerns over the Australian region and comparison over SWWA is described in the unabridged report for Theme 1 from Ryan and Hope (2005) (http://www.ioci.org.au). Datasets were averaged over the same 10 by 10 degree boxes described earlier: that area includes four grid points in the case of HadSLP2 and 25 in the case of the reanalyses (using points on the boundaries). All three datasets exhibit an overall consistent increase of the order of 1 hPa during the common period from 1958 to 2003; however the curves do not match exactly and suggest differences in timing and magnitude of the MSLP increases which are worth investigating further.

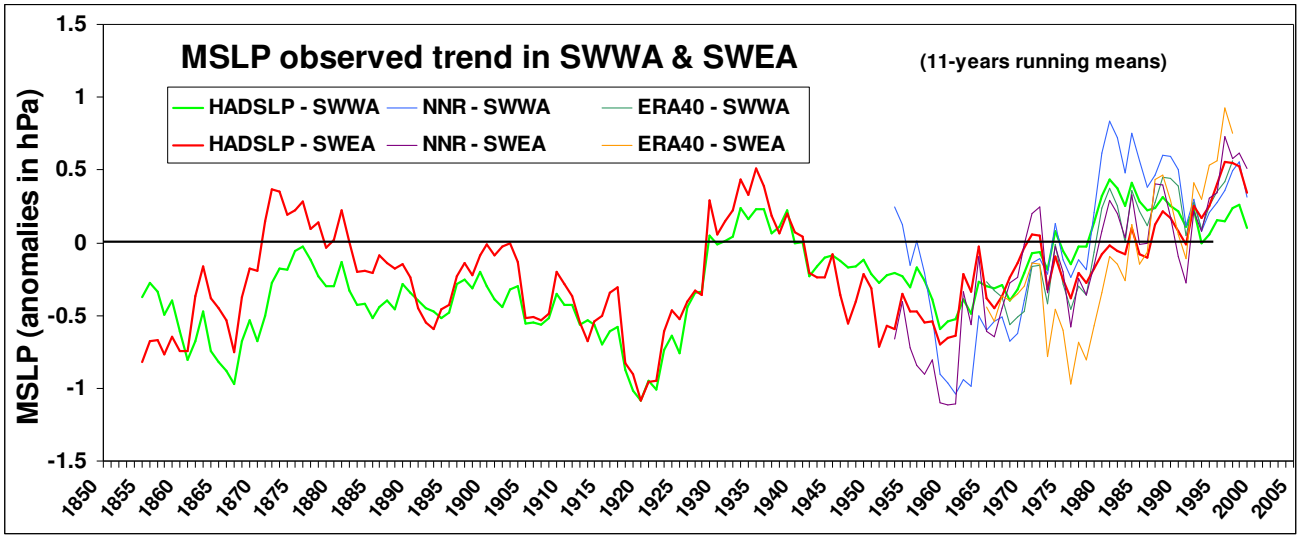

Figure 4. *11-year running mean of MJJ MSLP anomalies in SWWA and SWEA as shown by three datasets: HadSLP2, NNR and ERA40 over their respective record lengths. Anomalies are calculated from the 1958 to 2003 mean.*

There is an important discontinuity in the amount of data fed into the re-analyses around 1978-1979 when satellite information started to become available. Prior to 1978, reanalyses rely on a mix of observations from the surface, radio sondes, ocean buoys and boat or aircraft based observations. This addition of satellite data, while global, had a profound effect in the southern hemisphere, in particular at higher latitudes due to the scarcity of data prior to the satellite era. In order to assess the impact of the discontinuity on MSLP in the regions under consideration here, the two sets of reanalyses were compared for two periods either side of the discontinuity: 1958-1978 and 1980-2002. In addition HadSLP2 which relies only on surface observations and hence is not

affected by this particular step change is used as a benchmark.

Table 1. *Squared correlation between various MSLP datasets (ERA40, NNR and HadSLP2) in MJJ for both SWWA and SWEA over the common period: 1958 to 2002 and during two shorter periods: pre-satellite (1958 to 1978) and post-satellite (1980 to 2002).*

r^2	1958 to 2002		1958 to 1978		1980 to 2002	
	SWWA	SWEA	SWWA	SWEA	SWWA	SWEA
NNR&ERA	0.90	0.94	0.86	0.92	0.96	0.98
NNR&HAD	0.90	0.90	0.92	0.92	0.83	0.85
ERA&HAD	0.86	0.86	0.88	0.90	0.81	0.85

Correlations are calculated between all datasets over the entire common period and for the two sub-periods (Table 1). Squared correlations (or percentage of explained variance) are very high between the three products (above 0.86 for both regions). These numbers are consistent with global comparisons of HadSLP2 and ERA40 (Allan and Ansell, 2006). The correlations in the first and second halves of the period support the concerns with the data quality: the cpwdorrelation between the re-analyses increases in the latter period. But, the correlation between the surface observations-based (HadSLP2) dataset and model generated estimates (both sets of re-analyses) using all available observations including satellite data (and upper-air observations) decreases in all cases. This result is consistent with the general understanding that re-analyses are an enhanced product once satellite data are used. Furthermore, it suggests that as re-analyses become more reliable after 1979, they depart more from HadSLP2 for which the network of available observations, while improving (Figure 4), does not exhibit a spectacular jump.

One known data concern in NNR that may influence the interpretation of the correlations after the introduction of satellites is the error produced from the inclusion of synthetic MSLP data for the Southern Ocean being shifted by 180º longitude during 1979 to 1992 (http://www.cpc.ncep.noaa.gov/products/wesley/paobs/paobs_1.html). This error has a major impact on latitudes south of about 40ºS. The NNR were re-run (NCEP- Department of Energy (DOE) Atmospheric Modelling Intercomparison Project2 (AMIP-2) reanalyses, commonly termed 'NCEP2') to account for this, and other, errors. Hines *et al.* (2000) explore the biases that these errors introduced. To assess the level of influence that these errors might have on the trends in the regions considered here, correlations between NCEP2 and the other datasets were assessed. Squared correlations between NCEP2 and HadSLP2 are indeed higher than for NNR during the post 1979 period, suggesting that the extent of the influence on MSLP due to this error might extend into our regions of interest (Table 2).

Nevertheless, the best match between any reanalyses and the HadSLP2 is observed during the pre-satellite era. It is worth noting that looking at squared correlations with the other reanalyses, NCEP2 is almost indistinguishable with NNR and hence the bogus inclusion of observed MSLP appears to have less impact on the reanalyses than the assimilation of satellite data.

Table 2. *Squared correlation between various MSLP datasets (ERA40, NNR and HadSLP2) in May-June-July for both SWWA and SWEA and the NCEP2 for the post-satellite era (1980 to 2002).*

r^2	NNR		ERA40		HadSLP2	
	SWWA	SWEA	SWWA	SWEA	SWWA	SWEA
NCEP2	0.99	0.99	0.96	0.98	0.87	0.89

Table 3. *Linear trend (multiplied by n), variance (standard deviation) and normalised trend (linear trend divided by the standard deviation) in May-June-July calculated for three MSLP datasets (ERA40, NNR and HadSLP2) for SWWA and SWEA over the common period of all datasets: 1958 to 2002.*

	Trend		Variance		Normalised trend	
	SWWA	SWEA	SWWA	SWEA	SWWA	SWEA
NNR	1.63	1.26	1.93	2.24	0.84	0.56
ERA40	1.18	1.20	1.70	2.16	0.70	0.56
HAD	0.74	0.90	1.12	1.30	0.66	0.70

Linear trends over the common period 1958-2002 calculated with each dataset agree in sign, the magnitude is of the same order for both regions but differs from one dataset to another (left two columns in Table 3). Although the mean signal is very similar between all three datasets (Figure 3), the variability is noticeably lower for HadSLP2 compared with both reanalyses. The apparent smoothness of HadSLP2 was somewhat expected due to (1) the methodology employed to construct the gridded product (as discussed earlier) and (2) the coarser resolution. Nevertheless, the size of

the difference is somewhat unexpected. Both reanalyses exhibit an inter-annual variability about 70% larger than HadSLP2; NNR has the larger of the reanalyses (Table 3, middle two columns). In order to remove the influence of the different inter-annual variability on the trends, the trends were *"normalised"* (i.e. divided by the standard deviation of the series). This normalisation goes a long way toward reducing the differences in the trend magnitude between datasets, which now appears in close agreement over the entire common epoch from 1958 to 2002 (Table 3, right two columns).

Table 4. *Normalised trend (linear trend divided by the variance) in May-June-July calculated for four MSLP datasets (ERA40, NNR, NCEP2 and HadSLP2) for SWWA and SWEA over the pre-satellite era: 1958 to 1978 and post-satellite era: 1980-2002.*

	1958 to 1978		**1980 to 2002**	
	SWWA	SWEA	SWWA	SWEA
NNR	0.74	0.25	-0.04	0.48
ERA40	0.31	-0.36	0.45	0.78
HadSLP2	0.58	0.09	-0.16	0.91
NCEP2	N/A	N/A	-0.03	0.61

In order to account for the earlier occurrence of a rainfall decline (in the late 1960s) in SWWA compared to SWEA (mid 1990s), it is interesting to split the calculation of the linear trend in two halves (before and after the 1979 discontinuity, Table 4). NCEP2 was also used in the latter period. The normalised trends over these shorter periods are very different between the two regions. In SWWA for NNR and HadSLP2 most of the MSLP increase occurred during the 1960s and 1970s, with minimal trend in the latter period. While in SWEA, the opposite is true: the large positive trends are in the latter period, during the 1980s and 1990s. While this general finding is encouraging as it is consistent with the rainfall signal, it is noticeable that the agreement between the MSLP datasets that was arguably strong (once trends were normalised) over the entire period from 1958 to 2002 is not seen on these shorter periods with large positive trends visible in ERA40 in the latter period for SWWA and trends of conflicting sign in SWEA in the early period. Bromwich and Fogt (2004) found that winter data from both reanalyses must be considered with caution for the period prior to 1979: Comparisons with Hobart in the SWEA region and Perth in the SWWA region revealed that both reanalyses had similar levels of error, although ERA40 had higher levels of error in other regions of the Southern Hemisphere mid- and high- latitudes. Thus the weakly positive trends from HadSLP2 and NNR over the 1958-1979 periods in SWEA might be the most representative of reality rather than the negative trend of ERA40. Therefore any analysis of the rainfall-MSLP relationship requires care as it is likely to be dependent on the MSLP dataset used and it does not appear that a single "truth" exists.

Conclusions

Long-term (over 150 years) and more recent (since 1958) MSLP anomalies and trends were analysed for MJJ in several boxes relevant to the rainfall declines observed in southern Australia. Based on the longest record used, the HadSLP2 dataset, starting from 1850, currently MSLP anomalies are the highest on record (in particular for SWEA). There was however some concern about data quality in the early part of the record as available data are very sparse, although it is suggested that within the latitude bands relevant to southern Australian climate (30ºS to 45ºS) the dataset is of sufficient quality to justify examining inter-decadal trends over the longer term. For the second part of the 20th century, a careful comparison of HadSLP2 with three sets of reanalyses shows an overall coherent picture. MSLP has trended upward over southern Australia. These upward trends appear to have begun earlier over SWWA than over SWEA, which is consistent with the difference in timing of the rainfall decline in both regions. Differences were noted between the different MSLP datasets on shorter timescales but the conclusions mentioned above were robust across all three datasets.

Acknowledgements

This communication arises from the involvement of BT in the South-Eastern Australian Climate Initiative (SEACI) and PH in the Indian Ocean Climate Initiative (IOCI), the leading climate variability and climate change research programs focusing on the two regions used here. The support of these projects is acknowledged. Eun-Pa Lim (BoM/CAWCR) prepared the NCEP2 dataset for us and made useful comments as did Peter Steinle (BoM/CAWCR) on this note.

References

Allan, R. and Ansell, T., 2006: A newly globally complete monthly historical gridded mean sea level pressure dataset (HadSLP2): 1850-2004, *J Climate*, **19**, 5816–5842.

IOCI, 2002: Climate variability and change in south west Western Australia, *Tech. rep.*, Indian Ocean Climate Initiative Panel, Perth, 34 pp.

Kalnay, E., *et al.*, 1996: The NCEP/NCAR 40-year reanalysis project, *Bull Amer Meteor Soc*, **77**, 437–471.

Marshall, G., 2003: Trends in the southern annular mode from observations and reanalyses, *J Climate*, **16**, 4134–4143.

Murphy, B. and Timbal, B., 2007: A review of recent climate variability and climate change in south-eastern Australia, *Int J Climatol*, **28(7)**, 859-879

Hope, P., Timbal, B. and Fawcett, R., 2009: On the relationship between rainfall variability in the southwest and southeast of Australia on daily and longer time-scales, *Aus. Met. Mag.*, submitted.

Peixoto, J. and Oort, A., 1991: *Physics of Climate*, American Institute of Physics, 335 East 45th Street, New York 10017, ISBN 0-88318-712-4.

Ryan, B. and Hope, P. (Eds), 2005: Indian Ocean Climate Initiative Stage 2: Report of Phase 1 Activity; 2003- 2004. 40pp

Timbal, B. and Jones, D., 2008: Future projections of early winter rainfall in South East Australia using a statistical downscaling technique, *Clim Change*, **86**, 165-187.

Uppala, S., *et al.*, 2005: The ERA-40 re-analysis, *Quart J Roy Meteor Soc*, **131**, 2961–3012

Climate Change and Birds: a southern hemisphere perspective

Lynda E. Chambers

Centre for Australian Weather and Climate Research

Bureau of Meteorology

L.Chambers@bom.gov.au

Introduction

Temperature, rainfall and other climate variables influence species occurrence, range, boundaries and behaviour (e.g. Böhning-Gaese & Lemoine 2004). Climate can also influence the timing of natural events, such as migration, breeding and moult, as well as the availability of food sources, such as seeds, flowers, insects and other prey items (e.g. Dunn, 2004; Lehikoinen *et al.*, 2004).

Australia and Africa are large continents with a wide variety of climate zones, from arid to tropical to temperate (Figure 1). Over much of these continents winter conditions are not severe. In Australia this means that much of the avifauna is either sedentary or moves only short distances, generally less than 1000 km from their breeding grounds, in response to changing seasons or rainfall (Chan, 2001), though there are some notable exceptions, e.g. some duck species, seabirds and waders.

This paper looks at how the climate of Africa and Australia has changed, projected changes in climate, and gives examples of what this means to the avifauna of the region.

Our Climate Is Changing

We are currently experiencing a period of rapid environmental change. Over the period 1906 to 2005 global surface temperatures rose by 0.74ºC (Bernstein *et al.*, 2007). Although most regions of the globe warmed, the warming did not occur in a uniform way, with larger increases observed over higher northern latitudes than elsewhere. Land temperatures rose faster than ocean regions and, consistent with this warming, sea-levels rose and snow cover decreased (Bernstein *et al.*, 2007).

Changes have also been observed in global rainfall patterns. In the African and Australian region, significant decreases in precipitation occurred since 1900 in the Sahel, southern Africa and in the south west of Australia. In equatorial Africa and the north west of Australia precipitation increased over the period 1900 to 2005 (Bernstein *et al.*, 2007). With increased temperatures and reduced rainfall over much of Africa and Australia the area affected by drought is also likely to have increased (Bernstein *et al.*, 2007; Hennessy *et al.*, 2008).

Projected Climate Change

Global mean temperature is projected to continue to rise, with an increase of around 0.2ºC per decade projected for a wide range of emissions scenarios for the next two decades (Bernstein *et al.*, 2007). After this point, the rate of temperature increase is highly dependent on specific emissions scenarios. Other projected changes include: warmer and fewer cold days and nights and warmer and more frequent hot days and nights over land areas and an increased frequency of heatwaves and heavy precipitation (Bernstein *et al.*, 2007).

Projections for high latitudes and some tropical wet areas are for increased water availability and annual river runoff. However, for some of the dry regions of the tropics and mid-latitudes, and the semi-arid areas of southern Africa, annual river runoff and water availability are projected to decrease (Bernstein *et al.*, 2007).

Expected Impacts on Bird Species

Bird species and their communities are likely to be affected both directly and indirectly by changes in temperature, rainfall, CO_2 and changes in the frequency and intensity of extreme weather events. Climate is also expected to indirectly influence avian species through

interactions with other species, including prey items, vegetation, competitors, and humans, as well as through interactions with other processes, such as changed fire regimes.

There are a number of ways in which species are expected to respond, or adapt, to changes in climate (Chambers *et al.*, 2005), as summarized below.

Changes in distribution – latitudinal and altitudinal
To maintain their current climatic conditions species may need to move either upwards or poleward as temperatures increase. For montane species, the distance they need to travel may be relatively short, as temperature can decrease quite rapidly with altitude. However, many species in Australia and Africa may be limited by existing mountain heights, rapidly running out of suitable habitat, resulting in populations becoming geographically isolated. For the wide flat arid regions of Australia, and parts of Africa, the distances species would need to move to maintain their current climatic conditions would be very large. Habitat fragmentation and suitability will limit species movements. For coastal breeding and feeding species, sea-level rise is expected to push species inland.

Changed movement patterns
As temperatures increase, some species that currently migrate between habitats are expected to either shorten their migration distance or stop migrating altogether, becoming year-round residents. Alterations of resources in time and space may also change the movement patterns of nomadic species, particularly waterbirds.

Phenology – life cycle timing
Temperature is an important cue for many phenological events, such as migration and breeding timing. In more arid regions, rainfall is also an important cue. As temperatures increase and rainfall patterns alter, changes are expected in the timing of migration and breeding (e.g. pair formation, egg laying, incubation length), moult, etc. Timing of these events can influence the reproductive success, survivorship and fitness of a species.

There are concerns that some bird species may mismatch their migration and/or breeding timing with that of their food sources, particularly in the case of long-distance migrants who may initiate their migration according to photoperiod, whereas peak abundance of their food sources may vary according to local temperature or rainfall signals.

Change in abundance (including local extinctions)
Under most climate change scenarios many species populations are expected to reduce and become fragmented and local extinctions may result. This could be due to direct mortality associated with climatic extremes or reduced reproductive success. Reductions in population size can reduce a species genetic diversity and other threatening processes, such as habitat fragmentation, may magnify the impact.

Physiology, morphology and behaviour
As global temperatures increase, changes may occur in the morphology of bird species, such as a decrease in body size (Bergmann's Rule). Species may need to alter their physiology, morphology, or behaviour, or combinations of these, to maintain body temperature and adapt to a changed water balance.

Community composition
Species-species contractions and expansions in range, changes in abundance of some species and habitat types, together with alterations in phenology, will result in new species interactions and changes in the structure and composition of present-day communities.

Indirect effects
Species may be indirectly affected via climate-related impacts on other species and various aspects of their habitat and food supply. Climate change is expected to directly impact vegetation, via changes in temperature, rainfall, fire regimes and atmospheric CO_2 and this may affect the quality and connectivity of bird habitat. Climate effects on the timing of flowering, fruiting and seeding of plants or the emergence of insects will affect the food supply of many bird species and other species on which birds depend.

Winners and Losers
Under a changing climate there are expected to be species that are able to adapt well and even prosper, while other species are expected to

suffer. Characteristics of species expected to do well are those with short generation times, that have good dispersal abilities, currently have broad climatic tolerances, are generalists and opportunists. In contrast, those with long generation times, are poorly dispersed, have narrow climatic tolerances, are specialists, have large home ranges, occur in isolated populations and are genetically impoverished are less likely to fair well under a changed climate.

Observed Changes

In 2007 the Intergovernmental Panel on Climate Change released their Fourth Assessment Report. Table TS.1 of the Working Group II report (IPCC 2007) highlighted the paucity of significant observed climate-related biological changes in the southern hemisphere: in fact 28,115 of the 28,671 biological systems listed were from Europe. It is a little uncertain as to the number of studies in both Africa and Australia, as the map and table disagree, though the number of studies is exceedingly small.

Since this report, additional studies have been published. Examples of which are given below.

Masked Lapwing

The Masked Lapwing (*Vanellus miles*) is a widespread species whose breeding distribution covers many Australian climate zones. A study by Chambers *et al.* (2008a) used the Birds Australia Nest Record Scheme (1957-2002) and Atlas of Australian Birds (1998-2006), both containing data generated by the general public, to look at spatial and temporal variation in breeding timing and success, particularly in relation to climate. Breeding records were analysed for six regions, as a compromise between having enough data in any one region for robust analyses and having regions small enough to capture climatic and habitat differences. Some differences were found over the breeding range of this species. In the more tropical and monsoonal north west, the birds bred mainly in summer, while in other regions breeding occurred during spring. Only Tasmania, in the temperate south, had significantly more breeding than the other regions. Breeding success also varied by year and region, with much higher breeding success in Tasmania. Tasmania was also the only region to see a significant change in breeding success over time (a decrease of ~1.5% per year). Some changes in breeding timing were seen in the north east (earlier by ~2 days per year) and in the south east (later by ~1 day per year). In terms of climate, all regions warmed, rainfall increased in the northwest and decreased in all eastern regions. For this species there were weak or no relationships between the temperature and rainfall and breeding, except in Tasmania. This species has a wide climate tolerance and appears to be fairly resilient to the changes in climate experienced so far.

Helmeted Honeyeater

The Helmeted Honeyeater is a critically endangered subspecies of the Yellow-tufted Honeyeater (*Lichenostomus melanops cassidix*), with a very restricted distribution in eastern Victoria, Australia. This species has been regularly monitored by the Victorian Department of Sustainability and Environment since 1989. Over this period, egg laying became earlier by ~1.4 days per year and the mean number of eggs laid per pair decreased by 0.012 eggs per year (Chambers *et al.*, 2008b). The study found that fewer eggs were laid in times of lower rainfall and that rainfall in this region was decreasing at ~21 mm/year. According to the relationships developed, egg laying is expected to become earlier under most climate change scenarios, however, this does not relate to increased breeding success in this species (Chambers *et al.*, 2008b).

Migration timing in south-eastern Australia

Using migration dates of south-eastern Australian birds sourced from published literature, Beaumont *et al.* (2006) looked at changes in arrival (24 species) and departure (12 species) timing. They found an average advance in arrival timing of ~3.5 days per decade and an average delay in departure of ~5.1 days/decade. The short- to middle-distance migrants tended to arrive earlier and depart later, extending the time they spent at their breeding grounds, while the long-distance migrants advanced both their arrival and departure dates, resulting in no change to the length of time spent at the breeding grounds (Beaumont *et al.*, 2006).

Migration timing in south-western Australia

This study used ~30 years of daily bird lists compiled by a single observer (Chambers, 2008).

Twenty species of water and land birds were identified as regularly departing and returning to the study site. Over, and prior to, the period 1973-2000 a significant reduction in rainfall was observed, as well as increased minimum temperatures. Of the 20 study species, 47% significantly altered their arrival timing and 41% altered their departure dates. The spring arriving species generally arrived earlier over time and had the strongest arrival trends, while autumn and winter arriving species generally arrived later over time. Changes in precipitation, rather than temperature, seemed to have the greatest influence of arrival and departure timing, particularly for the waterbirds (Chambers, 2008).

An African Example

Very few studies have looked at changes in migration or breeding timing of birds in the African region. The example below does so in an indirect manner by looking at the affect of temperature changes on arrival dates of two species of bird in the UK, who over-winter in Africa.

The Barn Swallow winters in western Africa, north of the equator, and departs for the UK in March. The Sand Martin winters in southern Africa, departing for the UK in late February/March. For both species arrival in the UK became earlier in recent decades, particularly for the Sand Martin, who now arrives earlier than the Barn Swallow (Sparks & Tryjanowski, 2007). Sand Martins appeared to be more temperature responsive than Barn Swallows and the marked change seen in the arrival timing of the Sand Martin may be a possible adaptation to the changed climate seen in recent decades (Sparks & Tryjanowski, 2007).

A number of recent studies have modelled changes in avian distributions and/or population dynamics under various climate change scenarios, for example, Erasmus *et al.* (2002), Okes *et al.* (2008), Wichmann *et al.* (2003) and Simmons *et al.* (2004), who projected range reductions for all six species studied.

Bridging the Knowledge Gaps

There is clearly a need for greater knowledge of how changes in climate can and will influence southern hemisphere species. In particular, there is limited information from Africa and over most of the Australian continent. We know very little about interactions that occur between species, even in the absence of climate change, or about interactions between climate change and other threatening processes, such as fire, land-use change and disease.

In Australia, a three-pronged approach is being trialed to help fill some of the knowledge gaps. This consists of:

- Searching: Documenting and analyzing existing long-term datasets. These can be hard to locate and it is useful to consider non-mainstream data sources (see below);
- Compiling: Searches of the literature and other sources to create new datasets. Other sources of data could include photographic records, egg collections, etc.
- Generating: The generation of new datasets through new monitoring programs, etc.

In all of these it is important to recognize the role that amateur naturalists can play in data collection.

Searching

The table below lists some recent Australian studies and the source of data used. These range from the use of government databases (e.g. Department of Sustainability and Environment monitoring records) to non-government organization databases (e.g. Birds Australia's Nest Record Scheme) to amateur naturalist records. Alternative data sources that could be considered include: waterbird counts, hunting records, museum records, State Department atlas records, amateur naturalist diaries/notebooks, etc.

We have also developed a database to keep track of known ecological datasets that may be useful for climate change impact studies (http://www.bom.gov.au/nemd).

Compiling

Published literature, particularly journals and newsletters from ornithological and naturalist groups, are a great source of historical records (phenological, breeding success, and range). Some alternative data sources include: egg collections (date and location of breeding events), bird strikes at lighthouses and road kills (may provide information on migration, if checked regularly enough), digital photographs are a great new source of data (providing information on phenological phases and time of the event), etc.

A recent Australian project, PhenoARC, is systematically searching the literature for historical phenological records. In the 10 months that the project has been running over 10,000 records have been sourced from over 960 references.

Table 1. *Recent Australian studies, incl. data sources.*

Study	*Data Source*	*Reference*
Breeding timing & success: Masked Lapwing	Birds Australia's Nest Record Scheme & Atlas of Australian Birds	Chambers *et al.*, 2008a
Breeding timing & success: Australian Magpie	Birds Australia's Nest Record Scheme & Atlas of Australian Birds, Canberra Ornithologists Group Garden Bird Survey, New South Wales Atlas	Gibbs, 2007
Breeding timing & success: Helmeted Honeyeater	Victorian Department of Sustainability and Environment monitoring records	Chambers *et al.*, 2008b
Migration timing: south western Australia	Daily bird lists of amateur naturalist	Chambers, 2008
Abundance, altitude, migration timing (mammals & birds)	New South Wales Atlas	Green & Pickering, 2002

Generating

In addition to ensuring that existing projects, such as bird atlases and nest record schemes, are maintained and/or invigorated, a new project is being developed for the Australian region. ClimateWatch aims to test the use of a dispersed observer network in Australia to gather data on biological responses to climate change by building on the success of similar systems in the northern hemisphere, such as the UK Phenology Network. Progress of the system can be monitored through [http://www.climate-watch.org.au].

Conclusions

Our climate is changing and birds are proving to be useful and popular indicators of change. Many bird species have responded by changing their phenology, productivity or distributions. Despite some recent studies documenting climate-related avian changes in the southern hemisphere, knowledge gaps persist. Most southern hemisphere studies have limited spatial coverage and do not consider climate-species relationships prior to the 1950s, when global temperatures began to rapidly rise. In addition, little is known about interactions between species or with other threatening processes, particularly under a changing climate. Given the enormity of the problem, it is critical that we reinvigorate past monitoring programs and initiate new ones, while reducing as many of the non-climate change threats as possible. Engaging the community is one way of achieving this. With greater global and community awareness of climate change it is time to learn from each other and to work together to better manage threats to our biodiversity.

References

Beaumont, L.J., McAllan, I.A.W. & Hughes, L. 2006. A matter of timing: changes in arrival and departure dates of Australian migratory birds. *Global Change Biology* **12**:1-16.

Bernstein, L., Bosch, P., Canzioni, O., *et al.* 2007. *Climate Change 2007: Synthesis Report: Summary for Policymakers: An Assessment of the Intergovernmental Panel on Climate Change.* Intergovernmental Panel on Climate Change, Cambridge University Press, UK. http://www.ipcc.ch/pdf/assessment-report/ar4/syr/ar4_syr_spm.pdf. Accessed July 24 2008.

Böhning-Gaese, K. & Lemoine, N. 2004. Importance of climate change for the ranges, communities and conservation of birds. In: Møller, A., Fielder W. & Berthold, P (eds) *Birds and Climate Change. Advances in Ecological Research* **35**. Elsevier, Amsterdam. Pp 211-236.

Chambers, L.E., Hughes, L. & Weston, M.A. 2005. Climate change and its impact on Australia's avifauna. *Emu* **105**: 1-20.

Chambers, L.E., Gibbs, H. & Weston, M.A. 2008a. Spatial and temporal variation in Masked Lapwing breeding.2008a. *Emu* **108**: 115-124.

Chambers, L.E., Quin, B.R., Menkhorst, P. & Franklin, D.C. 2008b. The effects of climate on breeding in the Helmeted Honeyeater. *Emu* **108**: 15-22.

Chambers, L.E. 2008. Trends in migration timing of south western Australian birds and their relationship to climate. *Emu* **108**: 1-14.

Chan, K. 2001. Partial migration in Australian landbirds: a review. *Emu* **101**: 281-292.

Dunn, P. 2004. Breeding dates and reproductive performance. In: Møller, A., Fielder W. & Berthold, P (eds) *Birds and Climate Change. Advances in Ecological Research* **35**. Elsevier, Amsterdam. Pp 69-87.

Erasmus, B.F.N., van Jaarsveld, A.S., Chown, S.L., Kshatriya, M. & Wessels, K.J. 2002. Vulnerability of South African animal taxa to climate change. *Global Change*

Biology **8**: 679-693.
Gibbs, H. 2007. Climatic variation and breeding in the Australian Magpie (*Gymnorhina tibicen*): a case study using existing data. *Emu* **107**: 284-293.
Green, K. & Pickering, C. 2002. A potential scenario for mammal and bird diversity in the Snowy Mountains of Australia in relation to climate change. In: Korner, C. & Spehn, E. (eds) *Global Mountain Biodiversity: Changes and Threats.* Springer-Verlag, Berlin. Pp. 241–249.
Hennessy, K., Fawcett, R., Kirono, D., Mpelasoka, F., Jones, D., Bathols, J., Whetton, P., Stafford Smith, M., Howden, M., Mitchell, C. & Plummer, N. 2008. *An assessment of the impact of climate change on the nature and frequency of exceptional climatic events.* CSIRO and Bureau of Meteorology, Melbourne.
IPCC. 2007. Summary for Policymakers. In: Parry, M.L., Canziani, O.F., Palutikof, J.P., van der Linden, P.J. & Hanson, C.E. (eds) *Climate Change 2007: Impacts, Adaptation and Vulnerability. Contribution of Working Group II to the Fourth Assessment Report of the Intergovernmental Panel on Climate Change*. Cambridge University Press, Cambridge, UK. Pp 7-22.
Kottek, M., Grieser, J., Beck, C., Rudolf, B. & Rubel, F. 2006. World Map of the Köppen-Geiger climate classification updated. *Meteorol. Z.* **15**: 259-263
Lehikoinen, E., Sparks, T.H. & Zalakevicius, M. 2004. Arrival and departure in birds. In: Møller, A., Fielder W. & Berthold, P (eds) *Birds and Climate Change. Advances in Ecological Research* **35**. Elsevier, Amsterdam. Pp 1-31.
Okes, N.C., Hockey, P.A.R.& Cumming, G.S. 2008. Habitat use and life history as predictors of bird responses to habitat change. *Conservation Biology* **22**: 151-162.
Simmons, R.E., Barnard, P., Dean, W.R.J., Midgley, G.F., Thuiller, W. & Hughes, G. 2004. Climate change and birds: perspectives and prospects from southern Africa. *Ostrich* **75**: 295-308.
Sparks, T. & Tryjanowski, P. 2007. Patterns of spring arrival dates differ in two hirundines. *Climatic Research* **35**: 159-164.
Wichmann, M.C., Jeltsch, F., Dean, W.R.J., Moloney, K.A. & Wissel, C. 2003. Implication of climate change for the persistence of raptors in arid savanna. *Oikos* **102**: 186-202.

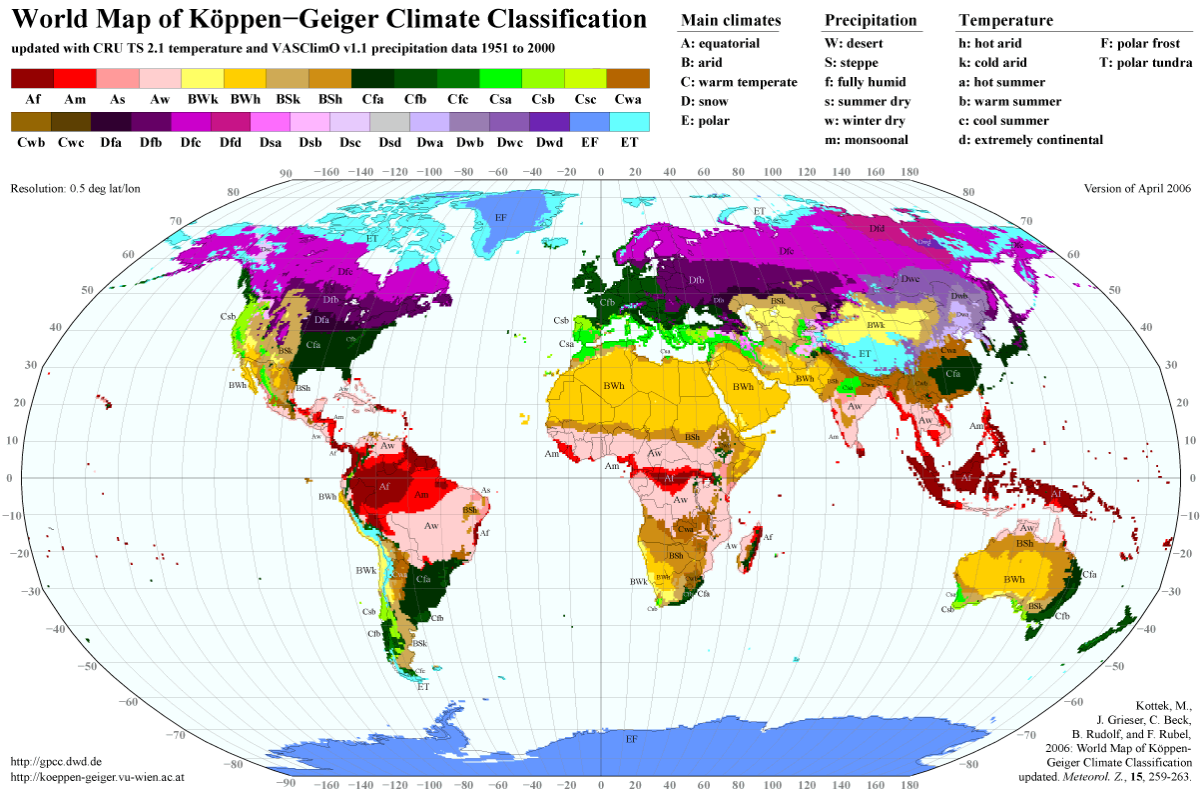

Figure 1. *Climate classifications of the world. Source: Kottek et al. (2006).*

East Australian Current and Tasman Sea Surface Drifting Buoy Experiment-2008

Gary B. Brassington[A], Nicholas Summons[B], Graeme Ball[C] and Lisa Cowen[D]

[A]Centre for Australian Weather and Climate Research

[ACD]Bureau of Meteorology

[B]University of Melbourne

g.brassington@bom.gov.au

Introduction

The East Australian Current (EAC) is a poleward western boundary current associated with the South Pacific Gyre (Boland and Church, 1981) extending from the Coral Sea to the Tasman Sea. The EAC develops from a bifurcation of the westward South Equatorial Current as it reaches the Australian coastline between 15S and 20S (Church 1987) and is observed to form a boundary current between 18°S and 35°S (Ridgway and Godfrey, 1994). The EAC separates from the boundary along the northern NSW coast to form mesoscale eddies and fronts in the Tasman Sea. The Tasman Sea is composed of many large, deep and long-lived eddies that interact with each other and the underlying complex bathymetry influencing the mean circulation (Tilburg *et al.*, 2001; and Ridgway and Dunn, 2003). A new approach to investigate the evolution of the circulation in this region has been the development of a multi-year ocean reanalysis in the Australian region (Oke *et al.*, 2008; Schiller *et al.*, 2008). The reanalysis represents the dynamical combination of information provided by an observing system including both in-situ and satellite data and a model estimated background state. In the present case this combination is provided by an Ensemble Optimal Interpolation scheme (EnOI, Oke *et al*, 2008; Evensen, 2003). Evaluating the quality of the reanalysis to aid in its interpretation as well quantifying its predictive skill for operational systems (OceanMAPS; Brassington, *et al.*, 2007b) is a critical activity. Surface drifting buoys provide an independent data set suitable for this purpose.

This research letter summarises the observations obtained from the 2nd East Australian Current and Tasman Sea Experiment conducted in Feb/Mar 2008. This experiment included 6 buoys deployed on three voyages as buoy pairs with a small initial separation. Deployments were made from two voluntary observing ships that operated along the PX30 XBT line from Fiji to Brisbane. The location where the XBT line transects the EAC is used to seed buoys into the EAC. The experiment was 100% successful at observing the EAC. This improved upon the experiment in 2007, where only one pair of buoys (out of 8) observed the EAC. The volunteer observers were instructed to deploy the buoys closer to the coast in 2008 compared with 2007. The buoy trajectories observe several features of the EAC, including the southward migration of the point of separation of the EAC and the formation of a coastal disturbance that induced a new point of separation for the EAC. The buoys were compared with OceanMAPS reanalyses to highlight instances of good agreement and regions of lower quality.

Deployments

The EAC and Tasman Sea experiment in 2007 (Brassington *et al.*, 2007a) successfully deployed eight buoys, however, only two buoys observed the EAC. This was determined to be due to the deployment location remaining too far to the east of the EAC. This was a conservative design decision to reduce the risk of buoys being entrained into the coast. The design for the 2008 experiment was modified to instruct the volunteer observers to deploy between 154.75°E to 154.5°E

and not west of 154°E. Six buoys were deployed during alternating crossings by the Forum Samoa II and Capitaine Tasman as described in Table 1.

Table 1. *A summary of the drifting buoy deployments during the experiment in 2008 based on the reports from the volunteer observers.*

Ship	WMO ID	Location	Date/Time
Forum Samoa II	55947	154 44.9 E 26 28.5 S	10-02-08 1650 UTC
Forum Samoa II	55950	154 42.0 E 26 28.8 S	10-02-08 1705 UTC
Capitaine Tasman	55611	154 28.9 E 26 27.18 S	25-02-08 1018 UTC
Capitaine Tasman	55908	154 23.0 E 26 28.37 S	25-02-08 1041 UTC
Forum Samoa II	55951	154 44.7 E 26 28.4 S	14-03-08 1537 UTC
Forum Samoa II	55952	154 38.3 E 26 32.0 S	14-03-08 1548 UTC

All of the buoys were deployed in the longitude range of 154.38°E to 154.75°E, latitude range of 26.53°S to 26.45°S and between 10 February to 14 March 2008.

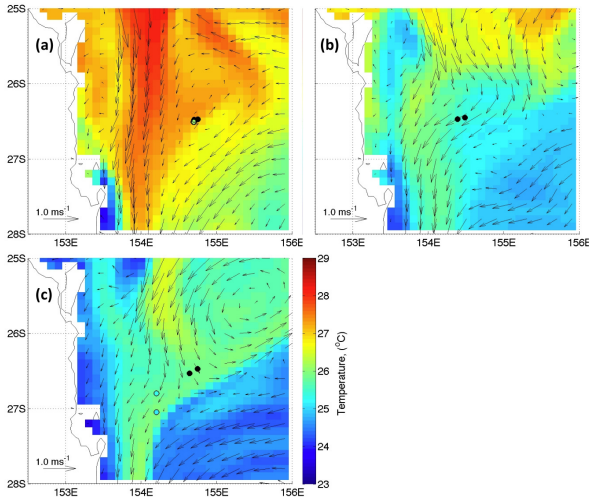

Figure 1. *Deployment locations from Table 1 shown as a solid marker (●) and overlayed on the sea surface temperature and surface currents estimated from OceanMAPS analysis for (a) 10 Feb, (b) 25 Feb and (c) 8 Mar, 2008. The first recorded observation is shown with a marker with face colour corresponding to the observed SST. Note that the first record for the second pair is outside the domain.*

The buoys were deployed as three pairs with an initial separation distance/time for each pair of (4.84 km/15 min), (10.0 km/23 min) and (12.5 km/11 min) respectively. All buoys were deployed on the open ocean side of the EAC in the ideal location for observing the EAC to avoid being entrained into the coastline. Overlaying the buoy positions on the surface fields estimated by BLUElink OceanMAPSv1.0b (Brassington *et al.*, 2007b) (see Figure 1) shows that the first pair was deployed in weak surface currents and the first observation occurred close to the deployment location. The second pair was deployed within a returning branch of the EAC and experienced large surface currents. The final pair was deployed near a temperature front and east of the peak EAC surface velocities.

The three buoy pairs observed the EAC current propagating along the coastline boundary between 26°S and 34°S (see Figure 2). The first two buoy pairs followed the coastline undisturbed until reaching the separation point. The final pair observed a transient disturbance that had formed at approximately 30°S which indicates an instability.

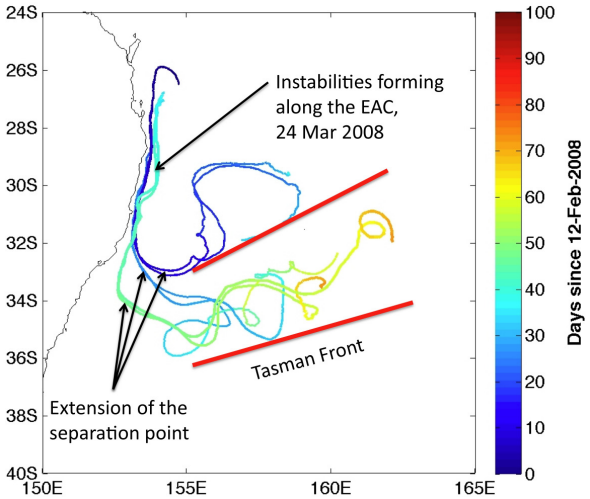

Figure 2. *The Lagrangian trajectory of the six drifting buoys defined by the first 500 recorded positions. The colour along the trajectory define the days since the first buoy record on 12 Feb 2008. The southward migration of the EAC separation point observed with each buoy pair is highlighted. The final buoy pair observed an instability forming off the coastline at ~30°S.*

This disturbance is visible as an SST anomaly discussed later and is linked to the premature separation of the EAC. The separation point is

observed to extend further south with each successive buoy pair. The first pair separate into a northern front. The remaining four buoys separate into a more classical Tasman Front.

The distance of buoy separation for the first pair (see Figure 3) shows a slower rate of growth indicating the buoys were in a similar streamline with reduced shear. The first pair also corresponded to the smallest initial separation at deployment. The second buoy pair began to separate rapidly at ~30°S, which is upstream of the eventual separation point from the coast. The increase in the distance of buoy separation is believed to be associated with increased shear across the EAC. After separating from the EAC, the second buoy separation distance grew rapidly (see Figure 2). The final pair showed a rapid growth in separation soon after initial deployment indicating the buoys were placed across a region of current shear. Figure 2 shows that the buoys traced a similar trajectory entrained within the EAC. The final buoy pair had the greatest initial deployment separation. It is noted however that subsequent to the EAC separation from the coast the buoys location converged to within 20 km, indicating they entered a region of slower flow rate and surface convergence.

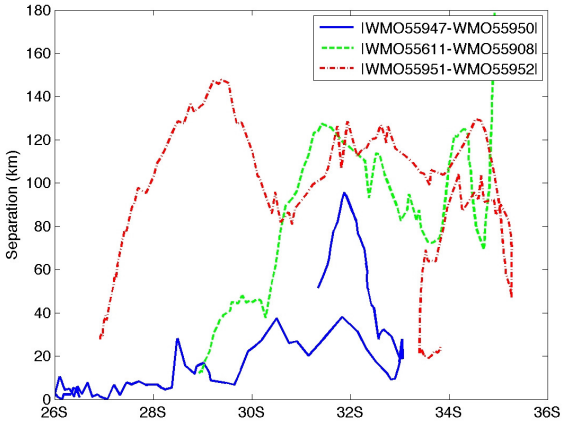

Figure 3. *Distance of buoy separation for each buoy pair relative to their mean meridional position. Distance of buoy separation is shown from first recorded observations until the buoys move away from the coastline.*

The surface currents estimated by the surface buoy positions (see Figure 4) showed high correlation during the first 30 to 40 days, which corresponded roughly to the period where the distance of separation was relatively small. The correlation reduced for each pair once the distance of separation grew, indicating the buoys were observing independent flow. The maximum current speed for each buoy pair is 2.3 ms^{-1}, 2.0 ms^{-1} and 1.8 ms^{-1} respectively, which occurs in the initial period whilst the buoys are within the EAC. The reduction in peak speed for each successive buoy pair could indicate the main EAC branch is decelerating but it could also be explained by the position of the buoys relative to the peak speeds of the current. The OceanMAPS analysis indicates that the small disturbance observed by the third buoy pair forms a new separation point and the main branch receives reduced volume transport. The third buoy pair also observed the EAC with speeds that oscillated in magnitude (see Figure 4c).

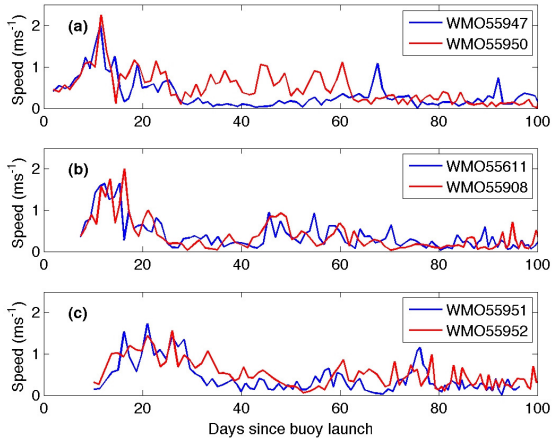

Figure 4. *Surface current speed estimated for each drifting buoy relative to the time since the first deployment over the first 100 days. (a) First, (b) Second and (c) Third buoy pair.*

Comparison with OceanMAPS

Comparison of buoy trajectories with OceanMAPS sea level anomalies suggest that the first buoy pair separated from the coast due to a cyclonic eddy that diverted the EAC offshore (see Figure 5a and 5b) forming a temperature front (not shown). The Lagrangian trajectory of this pair on 25 Feb 2008 indicates that the anti-cyclonic eddy to the north was more intense and positioned further to the south than is in the reanalysis. The observations of SST from the buoys are also warmer than those from OceanMAPS (not shown) further demonstrates that the separation point was located further to

the south. The sequence of SLA images in Figure 5 indicate the point of separation slowly propagated south. The dynamics of this type of propagation are not well understood and this feature was poorly constrained by the current ocean observing system. The first buoy pair then became attracted into a cyclonic eddy shown in Figures 5c and 5d. The shape of the eddy was not in perfect alignment with the estimated surface currents. Two additional surface drifting buoys in the region (one still active from the previous years experiment) observed the offshore front in Figure 5a matching closely the estimated surface currents.

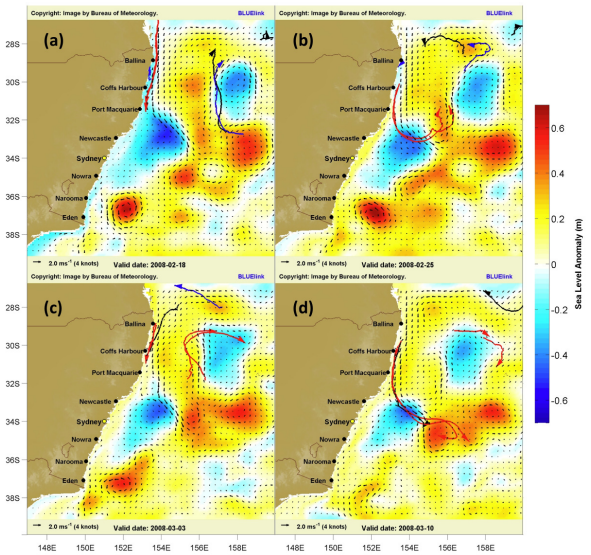

Figure 5. *The Lagrangian track for all surface drifting buoys in the region for a period of 9 days. This is overlaid on the OceanMAPS analysed ocean sea level anomaly and surface currents for the centred time. The buoy track are (red) experiment buoys deployed in 2008, (blue) still active experiment buoys deployed in 2007 and (black) all other buoys. Each image is separated by 7 days, (a) 18 Feb 2008, (b) 25 Feb 2008, (c) 3 Mar 2008 and (d) 10 Mar 2008.*

The second buoy pair (see Figure 5c) was joined by a third buoy that traced similar trajectories (see Figure 5d). Despite the presence of a cyclonic sea level anomaly to the south only the third buoy became attracted around the eddy (see Figure 6a). The corresponding observations of SST (not shown) from the same buoy were warmer than that estimated by OceanMAPS. The circulation pattern exhibited by the two experiment buoys (see Figure 6a) does not show good agreement with OceanMAPS, where both buoys show shorter radii of anticyclonic rotation than was estimated. The OceanMAPS analyses gave a complex pattern of sea level anomalies showing the model was undergoing eddy-eddy interactions that lead to relatively higher growth rates of forecast error. The altimetry coverage may not have been adequate to constrain the ocean state during these interactions.

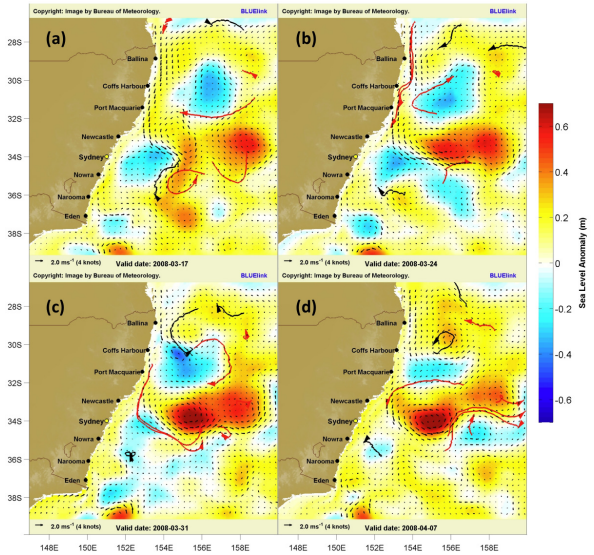

Figure 6. *Same as Figure 5 for (a) 17 Mar 2008, (b) 24 Mar 2008, (c) 31 Mar 2008 and (d) 7 Apr 2008.*

The third buoy pair (see Figure 6a and 6b) took approximately 9 days to propagate to the point of EAC separation at ~33°S. The position of separation was observed further south than what was estimated by OceanMAPS (see Figure 6c). The Lagrangian trajectories shown correspond more closely to the analysis in Figure 6d indicating it is likely that OceanMAPS was out of phase in propagating the front. The subsequent trajectories of the third buoy pair follow the front that was estimated in the analysis (see Figure 6d).

The EAC on 24 March 2008 (see Figure 6b) was not a continuous current having formed a small disturbance between Ballina and Coffs Harbour. The final pair of buoys both traced this feature, despite there being a significant distance of separation between the buoys at the time (see Figure 3). This indicates the disturbance was a robust ocean dynamical feature. OceanMAPS showed good agreement in the shape of the small coastal feature, as traced by the buoys, which

corresponded to a region of cooler SST (see Figure 7). The offshore cyclonic eddy with centre ~ (155°E, 31°S) (see Figure 6b) had formed a saddle point in the surface currents that was well traced by the buoy pair along the coast and the single buoy within the cyclonic eddy.

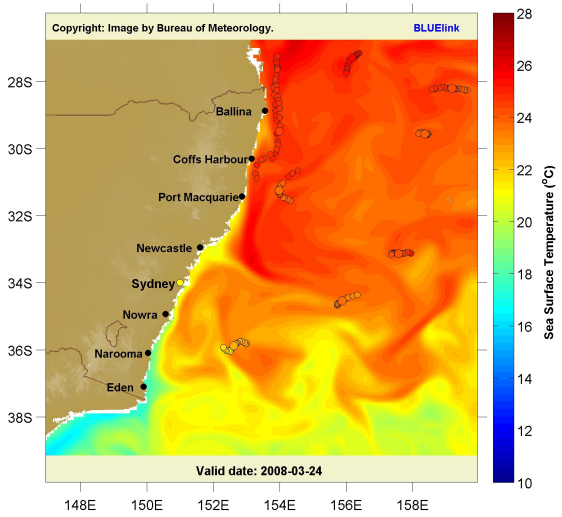

Figure 7. *The trajectories of buoys in the Tasman Sea represented by a series of markers coloured by the observed SST. The markers represent +/- 2 days from the central time, 24 Mar 2008. The marker corresponding to the central time is slightly larger. The markers overlay the OceanMAPS analysed sea surface temperature for 24 Mar 2008.*

Conclusion

The surface drifting buoy experiment conducted in 2008 was 100% successful at observing the EAC, indicating the robustness of the experiment design. The buoy pairs were able to confirm observed features and measure the dispersion properties of the EAC, including the low dispersion during the separation from the coast. The buoys observed the southward propagation of the EAC separation point and the formation of a coastal disturbance to the EAC between Ballina and Coffs Harbour. The OceanMAPS analyses of currents and positions of fronts showed many examples of good agreement with the observed trajectories of the buoys from the experiment and other buoys in the region. A particularly good example of this was the detection of the EAC disturbance and saddle point. However, there were also several examples where the OceanMAPS analysis showed poor agreement. One example is the time evolution of EAC separation position along the coast. This suggests the model has a slower propagation rate for this case. Another example is the small scale eddies observed by the buoys that do not agree with the analysed surface currents. Further detailed analysis of these observed features will continue to reveal their dynamics and predictability.

Acknowledgements

We gratefully acknowledge the captains, crews and volunteer observers aboard the Forum Samoa II and Capitaine Tasman; and Rick Lumpkin and NOAA for the supply and communications of the drifting buoys.

References

Boland, F. M. and J. A. Church, 1981: The East Australian Current 1978, Deep-Sea Res., **28**, 937-957

Brassington, G. B., N. Summons, G. Ball and L. Cowen, 2007a: East Australian Current and Tasman Sea pilot surface drifting buoy experiment, BMRC research letter, **6**, 21-26

Brassington, G. B., T. Pugh, C. Spillman, E. Schulz, H. Beggs, A. Schiller and P. R. Oke, 2007b: BLUElink> Development of operational oceanography and servicing in Australia, Journal of Research and Practice in Information Technology, **39**, 151-164

Church, J. R., 1987: East Australian Current adjacent to the Great Barrier Reef. Australian Journal of Marine and Freshwater Research, **38**, 671-683

Evensen, G., 2003: The Ensemble Kalman Filter: Theoretical Formulation and practical implementation, Ocean Dynamics, **53**, 343-367.

Oke, P. R., G. B. Brassington, D. A. Griffin and A. Schiller, 2008: The Bluelink ocean data assimilation system (BODAS), Ocean Modelling, **21**, 46-70

Ridgway, K. R. and J. S. Godfrey, 1994: Mass and heat budgets in the East Australian Current: a direct approach. J. Geophysical Res., **99**, 3231-3248

Ridgway, K. R. and J. R. Dunn, 2003: Mesoscale structure of the mean East Australian Current System and its relationship with topography, Prog. in Oceanogr., **56**, 189-222

Schiller, A., P. R. Oke, G. B. Brassington, M. Entel, R. Fiedler, D. A. Griffin, J. Mansbridge, 2008: Eddy-resolving ocean circulation in the Asian-Australian region inferred from an ocean reanalysis effort, Progress in Oceanography, **76**, 334-365

Tilburg, C. E., H. E. Hurlburt, J. J. O'Brien and J. F. Shriver, 2001: The dynamics of the East Australian Current system: the Tasman Front, the East Auckland Current, and the East Cape Current, J. Phys. Oceanogr., **31**, 2917-2943

Preliminary Evaluation of a Coupled Ocean-Atmosphere Prediction System

Paul A. Sandery[A] and Gary B. Brassington[B]

[AB]CAWCR Centre for Australian Weather and Climate Research,

Bureau of Meteorology, Melbourne, Australia

p.sandery@bom.gov.au

Introduction

Coupled weather forecasting for synoptic timescale processes in the Australian region has only recently become a practical problem to explore, with advances in computational possibilities, the introduction of the BLUElink ocean forecasting system (Brassington *et al.*, 2007; Oke *et al.*, 2008) and now the development of a coupled limited area model. It is well known that coupled models are essential for seasonal and climate prediction systems. More recently it has been demonstrated that they also tend to provide improvements in tropical cyclone intensity forecasting without degradation of track (Bender *et al.*, 2007). What is less clear is if there is any benefit to be gained by adopting coupled ocean-atmosphere models for synoptic scale weather prediction, since adding complexity and additional demands on computer resources may not justify the use of a coupled model for this application. To investigate this problem we have applied a coupled limited-area model to carry out a series of parallel NWP forecasts in the northern Australian tropical region. The coupled system uses the Bureau's tropical cyclone forecasting model TC-LAPS (Davidson and Weber, 2000), that runs as a regular LAPS model operationally issuing weather forecasts over the Darwin region (Figure 1) in the absence of the existence of a tropical cyclone. This instance of TC-LAPS is coupled to a regional version of the OceanMAPS-BLUElink operational ocean forecasting system and the coupled system is known as the coupled limited area modelling and prediction system (CLAM). The main application of CLAM is in studying the impact of coupling on tropical cyclone forecasts, however, the development of the system also provides the opportunity to investigate the coupled weather prediction problem. The region that is the focus of this study is shown in Figure 1.

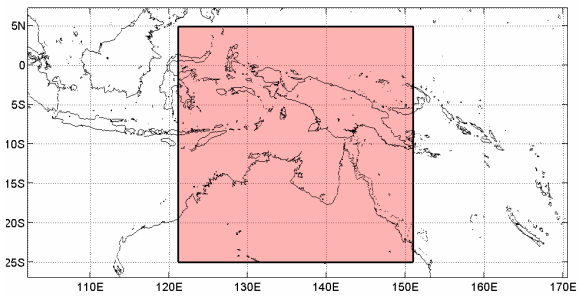

Figure 1. *Shaded area denotes coupled model domain covering the Northern Territory of Australia and various parts of the Coral and Indonesian Seas.*

An example of ocean initial conditions from OceanMAPS in terms of SST and some vertical temperature sections is given in Figure 2. SST time variability in this region is not large compared to other regions such as what might be expected in the East Australian Current region. An impression of the climate of regional SST variability can be seen in Figure 3 which shows the decorrelation timescale of SST derived from BRAN2.1 reanalysis data 1996-2006. Areas such as the Gulf of Carpentaria have relatively long decorrelation timescales up to 60 days suggesting low time variability. Areas of relatively higher SST variability have lower decorrelation timescales (5 – 25 days) such as in equatorial waters north of New Guinea, in the Indonesian Seas and Throughflow region as well as on the Australian northwest shelf and in the Timor Sea.

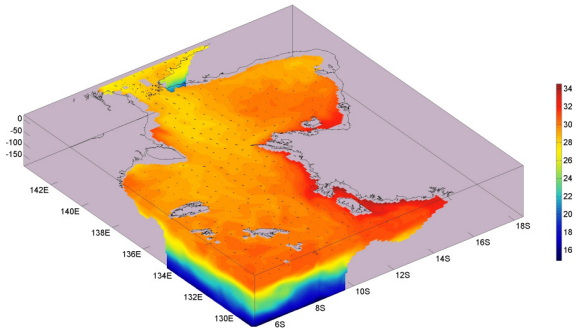

Figure 2. *Example of SST and vertical temperature sections from OceanMAPS that may be the boundary condition for a weather forecast in the region.*

One may not expect to see a large impact of coupling in a four day weather forecast if the coupled models were to only interact through SST in regions where SST variability is low. Furthermore, areas of relatively large heat content with deep warm mixed layers would in general require more work by the atmosphere to entrain cooler subsurface water to induce surface cooling. Coupling of currents to winds through an inertial coupling method may be more important in this region as there are periods of light winds that could coincide with relatively strong currents. This may have an important effect on the marine atmospheric boundary layer.

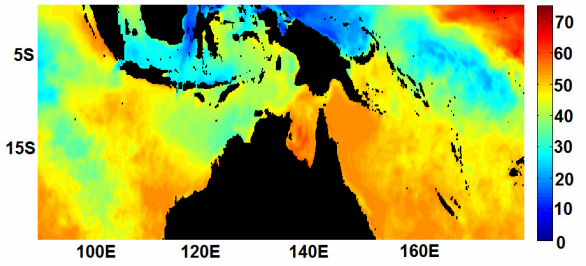

Figure 3. *Decorrelation timescale (days) of SST from BRAN2.1 ocean reanalysis 1996-2006.*

We suggest that including a more complete and accurate representation of sea-state, sea-surface temperatures and feedback processes that influence oceanic and atmospheric boundary layers, will lead to improvement in coastal and marine weather forecasts in particular. The trade off is between allowing physically based negative feedbacks from differential air-sea conditions versus uncertainties of exchange coefficients and feedback of errors.

The next section presents an outline of the system and a brief description of the methods is given. Following this, results from a coupled forecast are examined and the differences between this, the original forecast and the posterior analyses are presented.

System and Methods

The regional version of the BLUElink ocean model is based on MOM4p1. It has 1/10 degree horizontal resolution and 47 levels, the upper 20 resolving the vertical structure at 10 m resolution. Input data for initial and boundary conditions use analysis and forecast information from OceanMAPS. The first 24 hr period for the ocean and atmospheric models is treated as an initialization period where nudging to sea-level, currents, air temperature, surface pressure, mixing ratio and wind vorticity is performed. Both models are one-way nested inside their respective larger scale systems. The atmospheric model is TC-LAPSv4 with 0.1 degree resolution and 51 vertical sigma-levels. The ocean model and atmospheric model are coupled using OASIS3.1 (Valcke *et al.*, 2003). A certain sequence of analysis steps, provided in OASIS, is used to minimize extrapolation at model open boundaries and along coastal boundaries due to the fact that the atmospheric and ocean grids are not aligned. The coupling frequency adopted is 2 hrs whereby time-averaged fluxes are passed between the models. The exchanged variables in the coupled system are SST, surface heat fluxes, winds, currents and fluid densities. SST is calculated in the ocean model and is treated as surface skin temperature in the atmospheric model, even though, due to the ocean model vertical resolution, it is representative of a 10 m depth-averaged surface temperature. Surface heat fluxes from the atmospheric model are used to force the ocean model. An inertially coupled surface stress (Bye and Wolff, 1999) is shared by both the atmospheric and ocean model and is determined from relative differences in winds, currents and surface densities of the respective fluids. The method also accounts for the effects of the surface wave field through the stokes-drift velocity. This may only be a small effect in the region because the mean significant wave height (SWH) conditions are generally low (0.5-1m). Near Torres Strait and further east in the Coral Sea or further west in the Timor Sea, the mean SWH has larger magnitude (1-2m). This estimate is based on wave model analysis using ERA-40

(http://www.ecmwf.int/newsevents/meetings/workshops/2008/ocean_atmosphere_interaction/presentations/Belcher.pdf). Here, in the absence of a wave model we use a general estimate, based on observations, that the wave field stokes velocity is ~3% of the 18 m winds (Bye and Wolff, 1999).

The system is run in near real-time using input data from the most recently available ocean and atmospheric analysis-forecast cycle. The system began running routine coupled forecasts in September 2008 and since has been making about one forecast per week. Since a relatively small amount of forecasts have been carried out to date, we do not have statistically reliable information for a general result. In this paper we therefore focus on the details of one forecast (base time 20081027), and treat this as a twin experiment to examine sensitivities, in order to investigate the impact of coupling and validate the coupled forecasts with the corresponding operational NWP forecast and posterior analyses.

Results

Time series of wind speed components and surface and bottom model σ-level pressure, temperature and winds from the atmospheric model for a particular forecast at the Darwin AWS location are shown in Figure 4. Several different traces are shown due to the fact that two versions of TC-LAPS (v4 and v5) with different physics are being compared. In the legend in Figure 4 SLV represents data coming from surface fields, 3D represents data from model sigma-level closest to the surface. CLAM is the coupled model, TC-LAPSv5 is the current operational model and TC-LAPSv4 is the atmospheric model that has the same physics as the atmospheric model in CLAM. Independent runs with TC-LAPSv4 are carried out in order to test the impact of coupling, since this has the same physics as CLAM. The Analysis data comes from the operational system that uses TC-LAPSv5.

In order to see the impact of coupling, and the use of a different SST boundary condition, we performed an independent uncoupled run of TC-LAPSv4. Alternatively the difference between CLAM using TC-LAPSv4 and the operational TC-LAPSv5 will show the impact of coupling, of using different SST initial boundary conditions and whether the improved physics in the latter can be compensated for in the coupled model. In Figure 4 there is general agreement in the diurnal cycle and variation of all the quantities displayed, and it is not clear which model configuration performs better in terms of the analysis. This provides a general indication that the coupled model is in agreement with the NWP system, however, there are also differences that need exploration. Figures 5a and 5b illustrate the difference in the SST boundary condition between the coupled model and the operational model. This is essentially the difference between SST derived from OceanMAPS as an initial condition (that has been enabled to evolve according to model predictions of advection, horizontal diffusion, vertical mixing and heating/cooling due to surface heat fluxes) and the Bureau's regional Australian multi-sensor analysis (RAMSSA) SSTs that the operational model has as a fixed boundary condition for the duration of the forecast. The overall difference is that the mean SST from CLAM is about 1°C warmer than in the operational model.

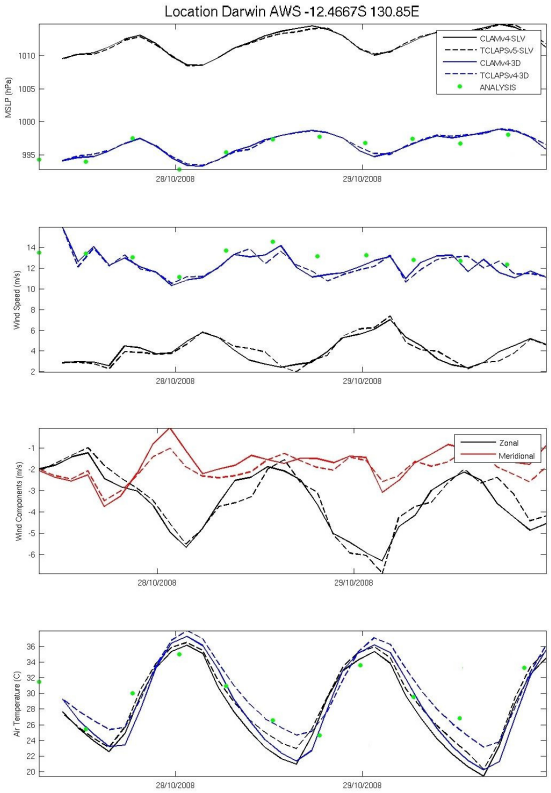

Figure 4. *Comparison of CLAM and various NWP forecasts at Darwin AWS station location in the model domain.*

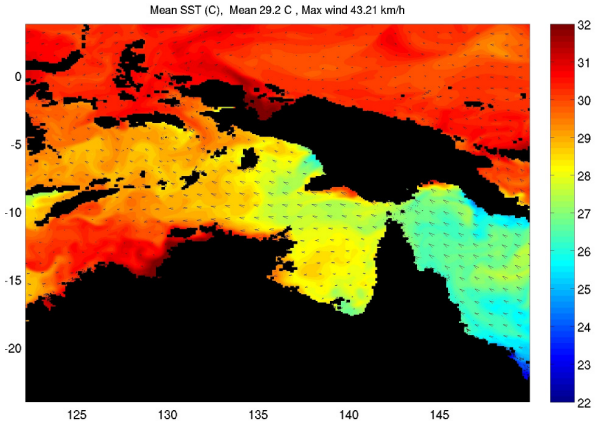

Figure 5a. *Mean CLAM SST for 96 hour forecast. Mean marine surface wind vector field also shown.*

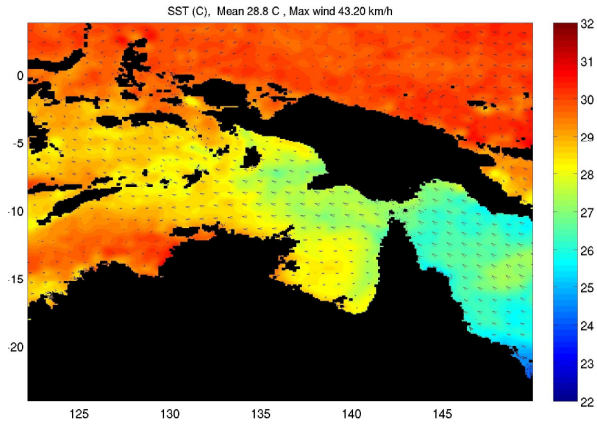

Figure 5b. *Fixed RAMSSA SST for 96 hour forecast. Mean marine surface wind vector field also shown.*

Figure 6 touches on the impact of coupling and using different SST boundary conditions in terms of the difference in mean wind speed between CLAM and TC-LAPSv4 (has same physics). Here in general, most of the differences occur over the ocean and in particular in coastal areas where SSTs are distinctly different between the two models. The effect of inertial coupling is highlighted in Figure 7 which shows the mean difference in winds between CLAM and the operational model for this particular forecast. Areas over the ocean where either relatively strong SST gradients or currents exist appear to be related to larger mean differences in wind speed. Noteworthy is the area north of New Guinea where it can be seen in Figure 8 that relatively strong westward surface currents dominate. Winds were approximately in the same direction at the time and with inertial coupling the relative stress was weaker resulting in reduced bottom friction experienced by the atmospheric model and stronger easterly winds.

The cool coastal biases in CLAM compared to the analysis could be suggesting a deficiency in the analysis in that is it not capturing details of coastal variation that are present in CLAM. Figures 9 and 10 compare CLAM and the operational NWP model with posterior analysis fields. RMS errors between model and analysis fields for winds and also surface air temperatures are about 10% lower in CLAM than in the operational forecast.

Also, strong land biases over New Guinea are significantly diminished in the coupled model yet there seems to be a warm bias compared to the NWP model over central Australia.

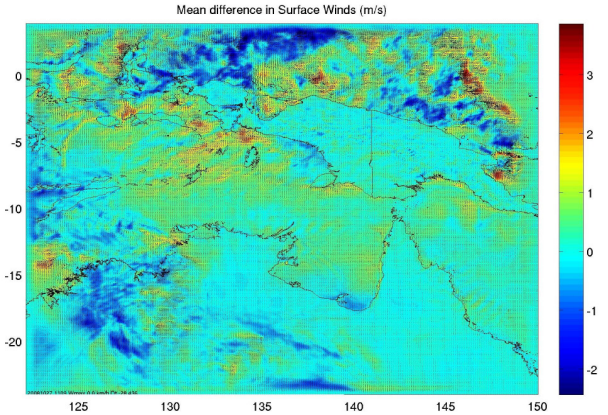

Figure 6. *Mean difference in surface winds in first 48 hrs of forecast between CLAM and TC-LAPSv4.*

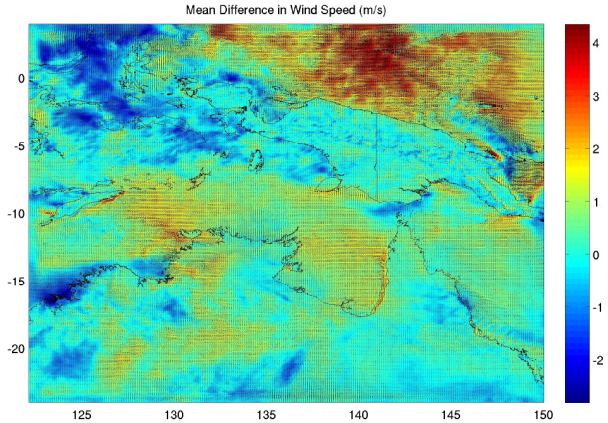

Figure 7. *Mean difference in surface winds in first 48 hrs of forecast between CLAM and TC-LAPSv5 operational NWP forecast.*

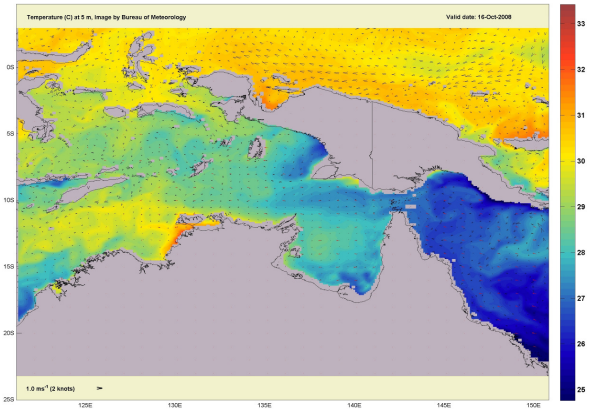

Figure 8. *Instantaneous CLAM SST (colour) and currents (vectors) at 48 hrs from forecast base time.*

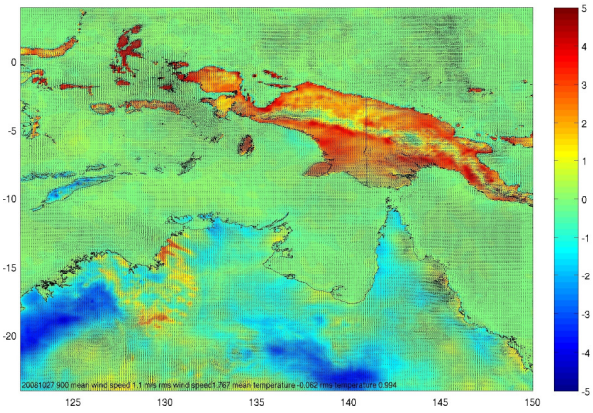

Figure 9. *Mean difference in surface air temperature and winds (vectors) between analysis and TC-LAPSv5 operational forecast over first 48 hours.*

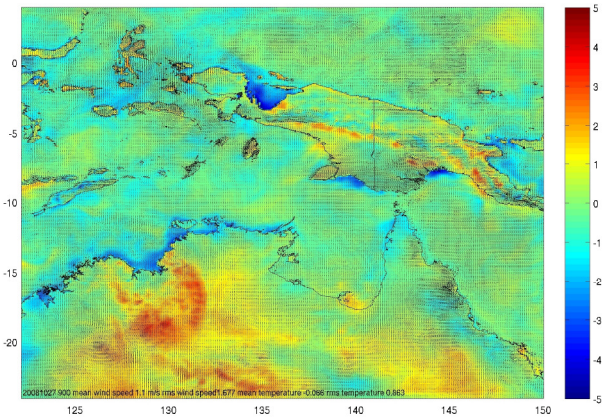

Figure 10. *Mean difference in surface air temperature and winds (vectors) between analysis and coupled forecast over first 48 hours.*

Conclusions

Results are presented that demonstrate the impact of air-sea coupling and initialization on a selected NWP forecast in northern Australia. Inspection of several other forecast runs indicate there are similar differences, such as larger winds over regions where winds are in alignment with strong currents and impacts of coastal SST gradients on local winds. The sensitivity of coupled weather simulations to SSTs modified by boundary layer dynamical processes and inertial coupling is demonstrated to be significant and warrant further investigation. The coupled model gave a significant improvement over the previous TC-LAPSv4 operational model and a slight improvement over the current operational model in terms of rms error in surface temperatures and winds compared to the post event analysis, although biases were spatially dependent and areas of inland Australia were less well predicted by the coupled model. This suggests that even though the current operational model has upgraded physics, the coupling is probably accounting for some of the physics missing in the previous version of the operational model, at least over the ocean part of the domain. Despite low SST variability there is a measurable sensitivity of the atmosphere to coupling. As the system continues to make routine forecasts, we will progressively be able to assess with clearer certainty the merits of ocean coupling for weather prediction in this region.

References

Bender, M.A., Ginis, I., Tuleya, R., Thomas, B. and Marchok, T., 2007. The Operational GFDL Coupled Hurricane-Ocean Prediction System and a Summary of its Performance. Monthly Weather Review, **135**: 3965-3989.

Brassington, G.B., Pugh, T., Spillman, C., Schulz, E., Beggs, H., Schiller, A. and Oke, P.R., 2007. BLUElink> Development of operational oceanography and servicing in Australia. Journal of Research and Practice in Information Technology, **39**: 151-164.

Bye, J.A.T. and Wolff, J., 1999. Atmosphere-Ocean Momentum Exchange in General Circulation Models. Journal of Physical Oceanography, **29**: 671-692.

Davidson, N.E. and Weber, H.C., 2000. The BMRC High-Resolution Tropical Cyclone Prediction System: TC-LAPS. Monthly Weather Review, 128: 1245-1265.

Oke, P.R., Brassington, G.B., Griffin, D.A. and Schiller, A., 2008. The Bluelink ocean data assimilation system (BODAS). Ocean Modelling, **21**: 46-70.

Valcke, S., Caubel, A., Declat, D. and Terray, L., 2003. OASIS3 Ocean Atmosphere Sea Ice Soil User's Guide, Technical Report TR/CMGC/03-69, CERFACS, Toulouse, France.

MALAPS and MesoLAPS: a case study of the East Coast Low event of 27th June 2007

M. Chattopadhyay[A], C. Vincent[B], J. Kepert[C]
[ABC]Centre for Australian Weather and Climate Research (CAWCR)
Bureau of Meteorology
700 Collins Street, Melbourne, VIC 3001

Introduction

Mesoscale assimilation and prediction systems are widely used to forecast boundary layer meteorology and associated phenomena. They are crucial for many applications, such as severe weather, fire weather and low level wind shear. BOM/CAWCR has recently taken keen interest in developing a mesoscale assimilation and forecast system for the above applications and to provide better wind prediction for wind energy applications. The new system is called MALAPS. We attempt to show that the research prototype MALAPS performed better than Bureau of Meteorology's (BOM) existing meso-scale prediction system during a severe weather event on the 27th of June 2007 which led to floods in Gippsland. It should be noted that the research prototype MALAPS has been operational since December 2007.

Description of the Assimilation and Modelling System

The assimilation system is based on the GenSI system (Steinle., 2005) developed in the BOM. The satellite radiances from NOAA 15, 16 and 17 available through UKMO's ATOVS data stream provides improved assimilation and prediction for the current system compared to the current operational systems (Harris *et al.*, 2005). In addition to the above satellite data, NASA's EOS Aqua AMSU-A microwave radiances, high density Atmospheric Motion Vectors (AMV) from geostationary satellite MTSAT and scatterometer marine wind vectors from QuikSCAT are also used in the assimilation system including data from all available *in-situ* systems. The cut-off time for the conventional data is 1 hour and 50 minutes and for ATOVS data the cut-off time is 3 hours. The numerical model was described by Puri *et al.* 1998 and here has a horizontal resolution of 0.10° and 61 levels up to 0.1 hPa in the atmosphere. MALAPS has 0.10° resolution topography derived from 30 second USGS data sets. The topography data is interpolated to the model grids. In addition, MALAPS has its land/sea mask adjusted by referencing back to the original topography dataset. No digital filtering is applied to the new system and Rayleigh friction is applied at the top most 6 layers of the model from 3 hPa to 0.1 hPa. The existing meso-scale prediction system in BOM, MesoLAPS, has a horizontal resolution of .125° and 51 levels in the vertical reaching up to 10 hPa in the atmosphere. The nesting configuration of MALAPS and MesoLAPS is depicted in Table 1.

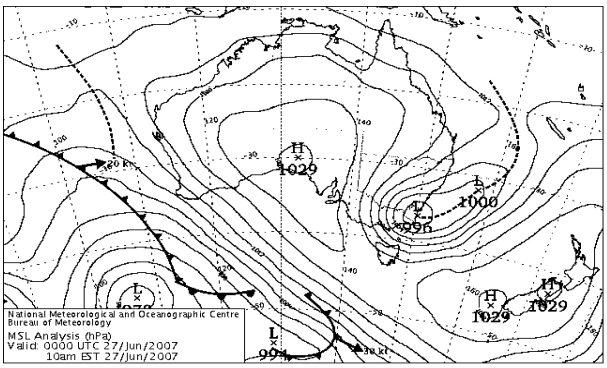

Figure 1 *Synoptic Situation for 20070627 00 UTC*

Table 1. *Research prototype (left) and then current operational (right) assimilation and forecast systems.*

Research prototype assimilation and prediction system	Operational assimilation and prediction system in June 2007
GASP_l60 Global Assimilation and Prediction System T_L239 (approximately 80 km), 60 levels, has its own analysis and forecast period up to 8 days	GASP Global assimilation and Prediction System T_L239, 33 levels, forecast period up to 8 days
LAPS-l61 Limited Area Assimilation and Prediction System 37.5 km horizontal resolution, 61 levels Forecast up to 72 hours	LAPS Limited Area Assimilation and Prediction System 37.5 km horizontal resolution, 51 levels Forecast up to 72 hours
MALAPS Meso-scale LAPS Assimilation and Prediction system 10 km horizontal resolution, 61 levels Forecast outlook to 48 hours	MESOLAPS Limited Area Prediction-only System 12.5 km horizontal resolution, 29 levels Forecast outlook to 72 hours

Study of 27th June 2007 East Coast Low

The east coast low event chosen for this study, which occurred on 27 June 2007, consisted of two low pressure centres that rotated around one another. The synoptic situation is shown in Figure 1. The first low centre made landfall near the southeast corner of the mainland, causing gale force winds and flooding in Gippsland, while the second centre remained offshore but brought an episode of gale force winds to the NSW coast. The AWS sites used for verification of this event are shown in Figure . The paths of the two low centres associated with this event are shown in Figure 2. The position of the model low centres were defined as the location of minimum pressure. The tracks of the systems in MALAPS and MesoLAPS are compared with the observed tracks, as located in the manual analysis from the BOM Victorian Regional Office. Both centres moved in a cyclonic path. Both NWP systems have the first low centre track too far to the west initially, but MALAPS has the landfall much further to the east than does MesoLAPS, in better agreement with the analysed track. The timing and position of landfall of the first centre is thus forecast significantly better by MALAPS than MesoLAPS, and this superior performance is reflected in the respective forecasts of MSLP and 10m wind speed as seen in Figures 4 and 5.

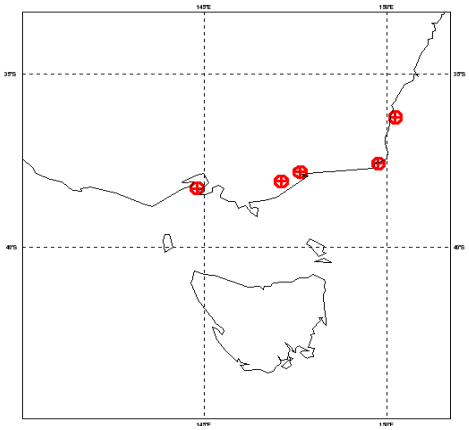

Figure 2. *AWS sites chosen to verify this event are: Montague Island, Mallacoota, Bairnsdale, East Sale and South Channel Island (ordered from right to left).*

The second low centre moved in a cyclonic path, and looped back over itself before heading south eastwards into the Pacific and dissipating. MALAPS and MesoLAPS predicted near identical paths for it, with both predicted the centre moving slightly too slowly and in too broad an arc. Analyses of MSLP from the two systems (Figure 4, left panels) show the low centre inland of Point Hicks, with the strongest pressure gradient in Bass Strait lying to the north of Flinders Island and impacting the coast between Lakes Entrance and Wilsons Promontory.

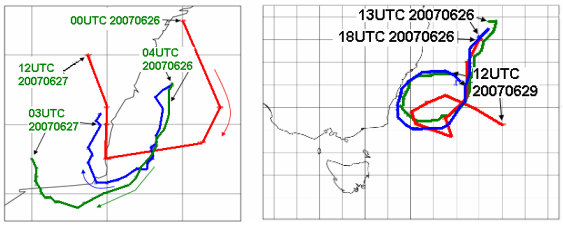

Figure 3. *East coast low tracks for the 20070626 East Coast Low. (left) First centre making landfall near the south east corner of the mainland. (right) Second low centre. Red: Observed (from manual analyses). Blue: MALAPS. Green: MesoLAPS.*

The MALAPS prognosis is quite similar, albeit

with the low pressure centre too close to the coast. In contrast, the MesoLAPS forecast has the low centre too far west, with the strongest pressure gradient south of Flinders Island and impinging on the northeast corner of Tasmania, and striking the Victorian coast to the west of Wilsons Promontory. The analysis (Figure 5) and forecast (not shown here) of 10-m winds are consistent with the MSLP field, with the MesoLAPS analysis having the arc of strongest winds too far to the south and west.

Note also that the MALAPS analysis displays considerably more fine-scale detail, consistent with its higher resolution. In summary, while neither analysis or forecast is perfect, it is clear that extreme winds are better located in MALAPS and this is borne out by the observations shown later in this the paper.

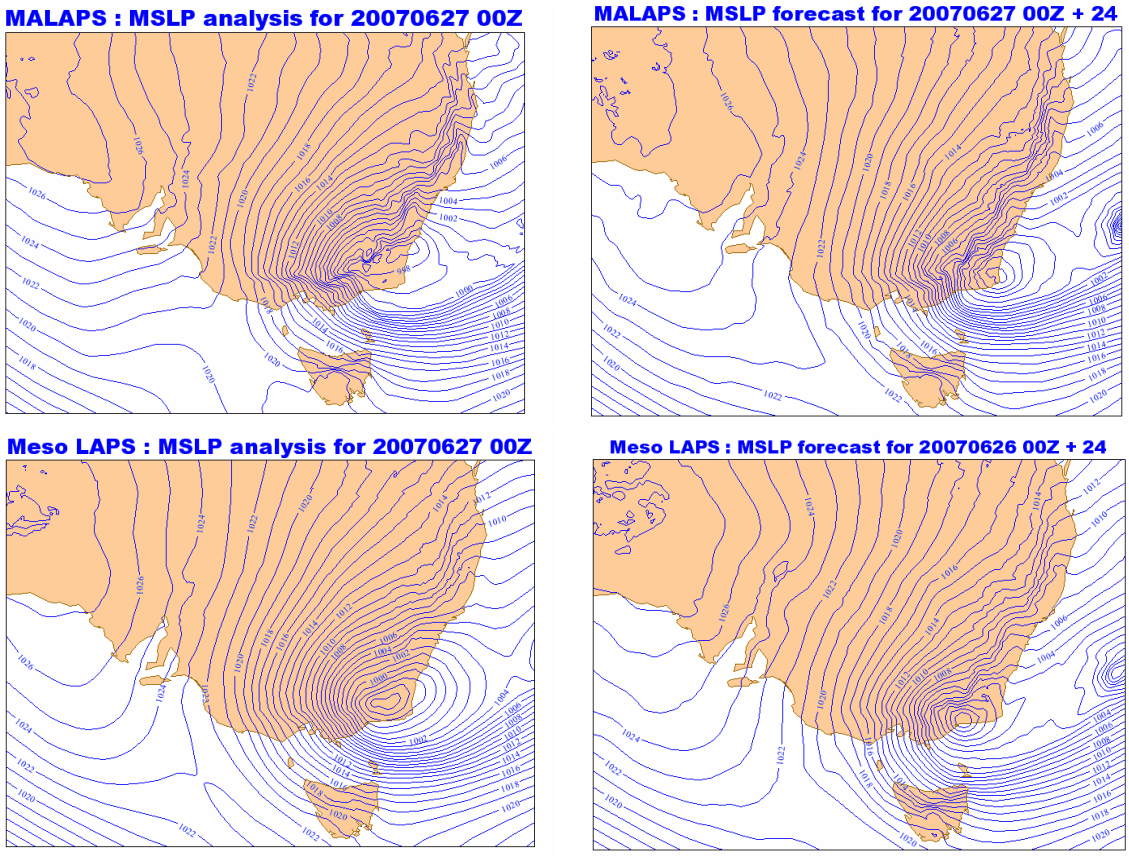

Figure 4. *Analysis and 24 hour prediction of MSLP for MALAPS (top) and MesoLAPS (bottom).*

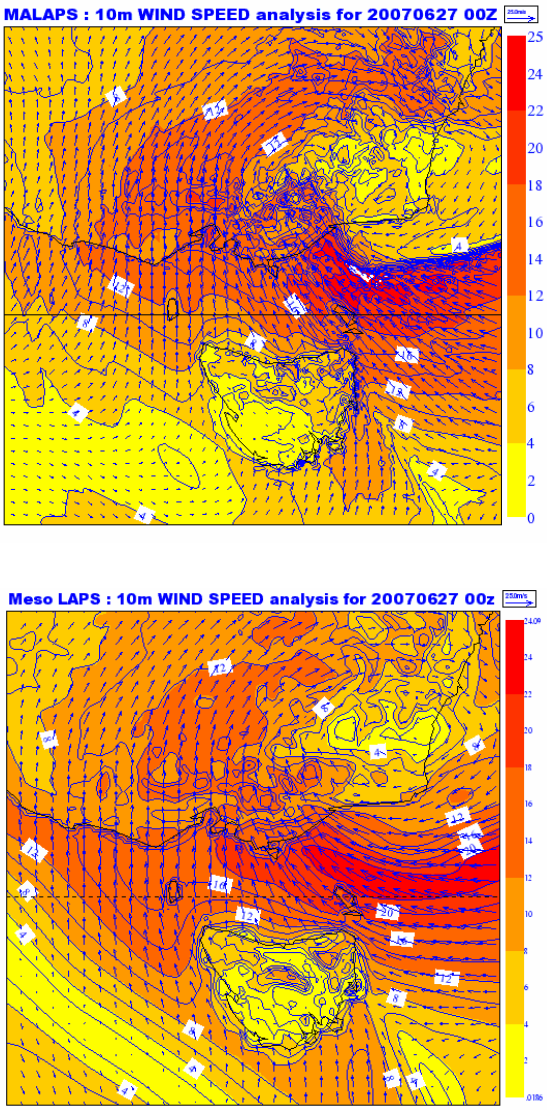

Figure 5. *Analysis of 10-m wind speed for MALAPS (top) and MesoLAPS (bottom).*

In order to diagnose the upper air structure of the two NWP systems their wind speed and temperature at 850 hPa and 500 hPa were studied in detail and found to be broadly similar for both the models. The vorticities of the two NWP systems were also analysed, and show some possibly significant differences. The MALAPS fields display a J-shaped band of high cyclonic vorticity extending to the northeast from the low complex. This is less well defined and broader in MesoLAPS, which also has a broad area of cyclonic vorticity to the north of the complex and (at 500 hPa) an arc extending around to the west. MesoLAPS also has some significant areas of anticyclonic absolute vorticity at 500 hPa (red and orange shading) that are absent or much weaker in MALAPS. These are an indication of inertial instability and may be unphysical. The most likely reason behind the differing depictions of vorticity may be the high-resolution assimilation in MALAPS of data including ATOVS and AMVs, whereas in MesoLAPS the physical parameters are interpolated from the coarser-resolution LAPS375 assimilation. The higher vertical resolution in MALAPS may also have contributed. It should also be noted here that MALAPS is nested in GASP-l61 and LAPS-l61 which performed better than the operational GASP and LAPS at that time. Hence, boundary conditions used in MALAPS may also have contributed to its better performance compared to MesoLAPS. A full diagnosis of the reasons for the different forecast low centre tracks between the models would be a difficult undertaking. Nevertheless, it is plausible to hypothesise that the marked differences in initial condition seen in these vorticity analyses may have contributed to the forecast differences.

Time-series of forecast and hourly observed wind speed for several AWS stations are shown in Fig 7. Overall MALAPS has done a better job in spot forecasts of 10m wind speed compared to MesoLAPS, due largely to its better forecast of the low track. For instance, the East Sale and Bairnsdale AWS time series plots in Figure 7 show the effect of the eye of the MesoLAPS forecast low crossing the coast at these sites, while the MALAPS forecast correctly predicted that the sites would be just westward of the low centre with correspondingly strong southeasterly winds. MALAPS has done a better prediction of the wind speed for the locations which are more to the west such as East Sale, South Channel Island and Bairnsdale than Montague Island Lighthouse and Mallacoota. The 36 hour time-series for Bairnsdale and East Sale in Figure 8 are plotted using observations from METAR data which have been used in the analysis cycle. It not only shows that MALAPS has successfully captured the timing of the front and predicted the wind speed but also captured the change in wind direction of the front better than MesoLAPS for both locations. MALAPS has also realistically predicted the change in the dry bulb and dew point temperature during the strong wind event.

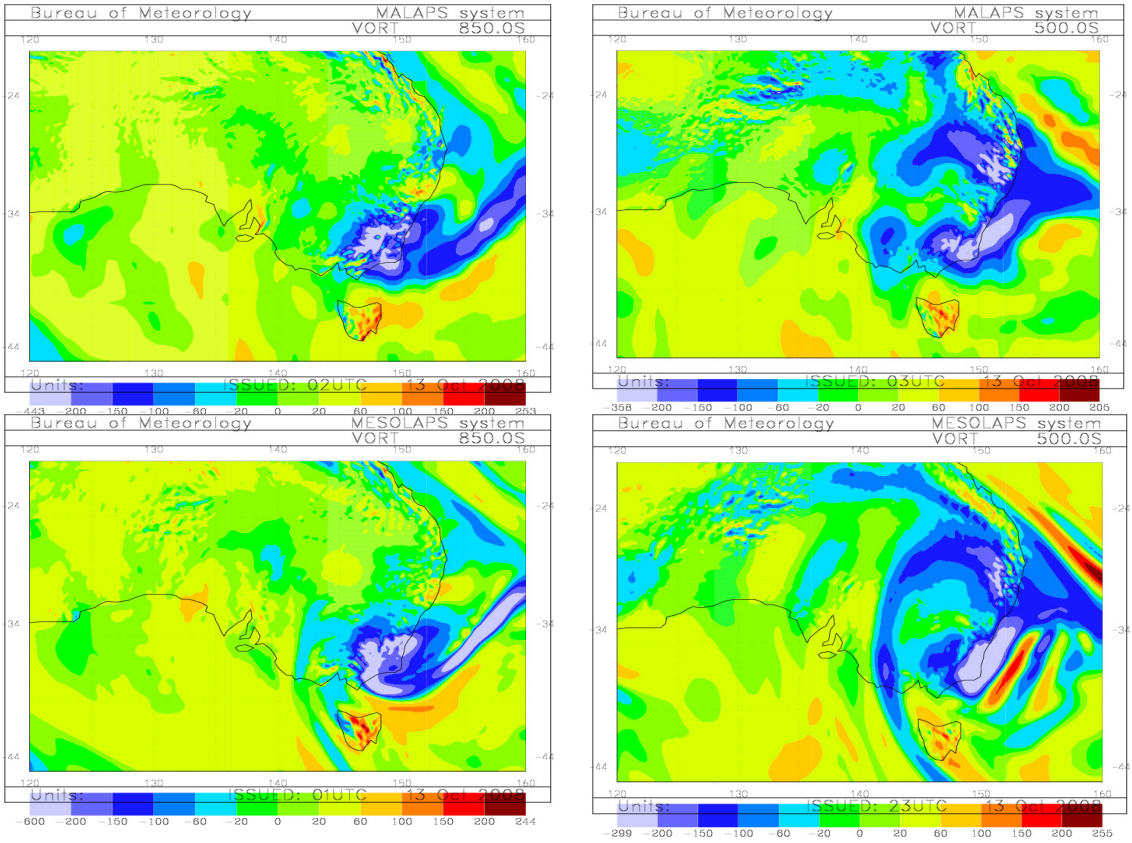

Figure 6. *850 hPa (left) and 500hPa (right) vorticity for MALAPS (top) MesoLAPS (bottom) at 2007062700. Units are 10^{-6} s^{-1}.*

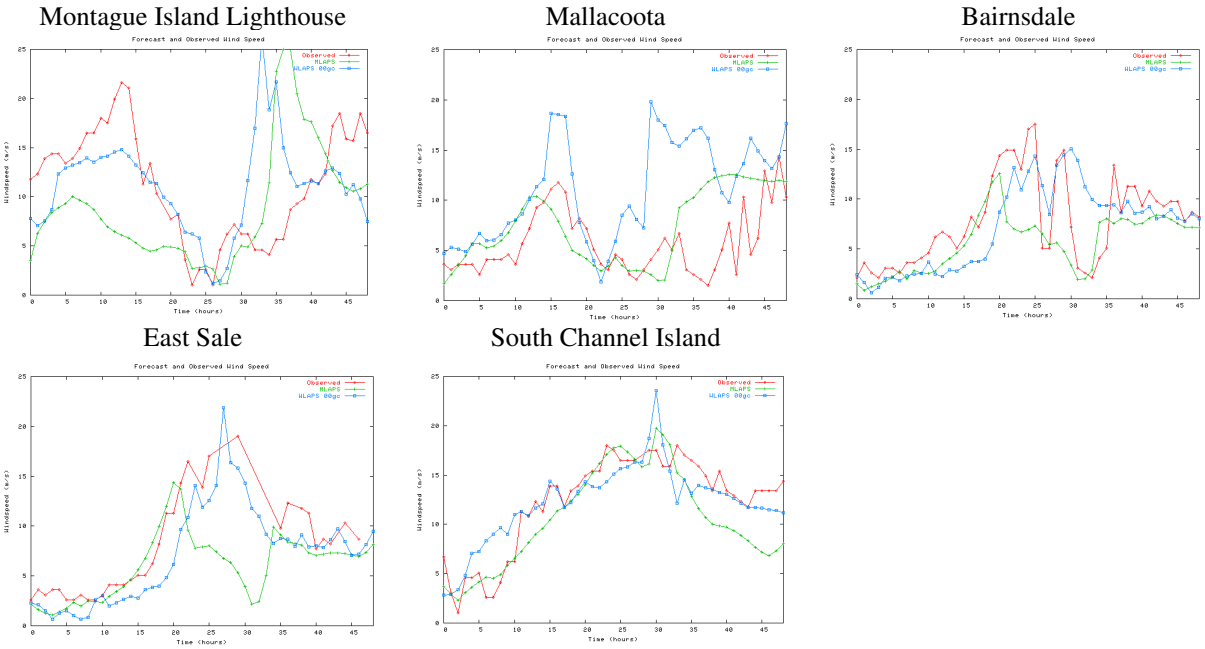

Figure 7. *Time series of 10m wind speed for the 48 hour forecast initiated 20070626 00UTC for Montague Island, Mallacoota, Bairnsdale, East Sale and South Channel Island. Red: Observed. Blue: MALAPS. Green: MesoLAPS.*

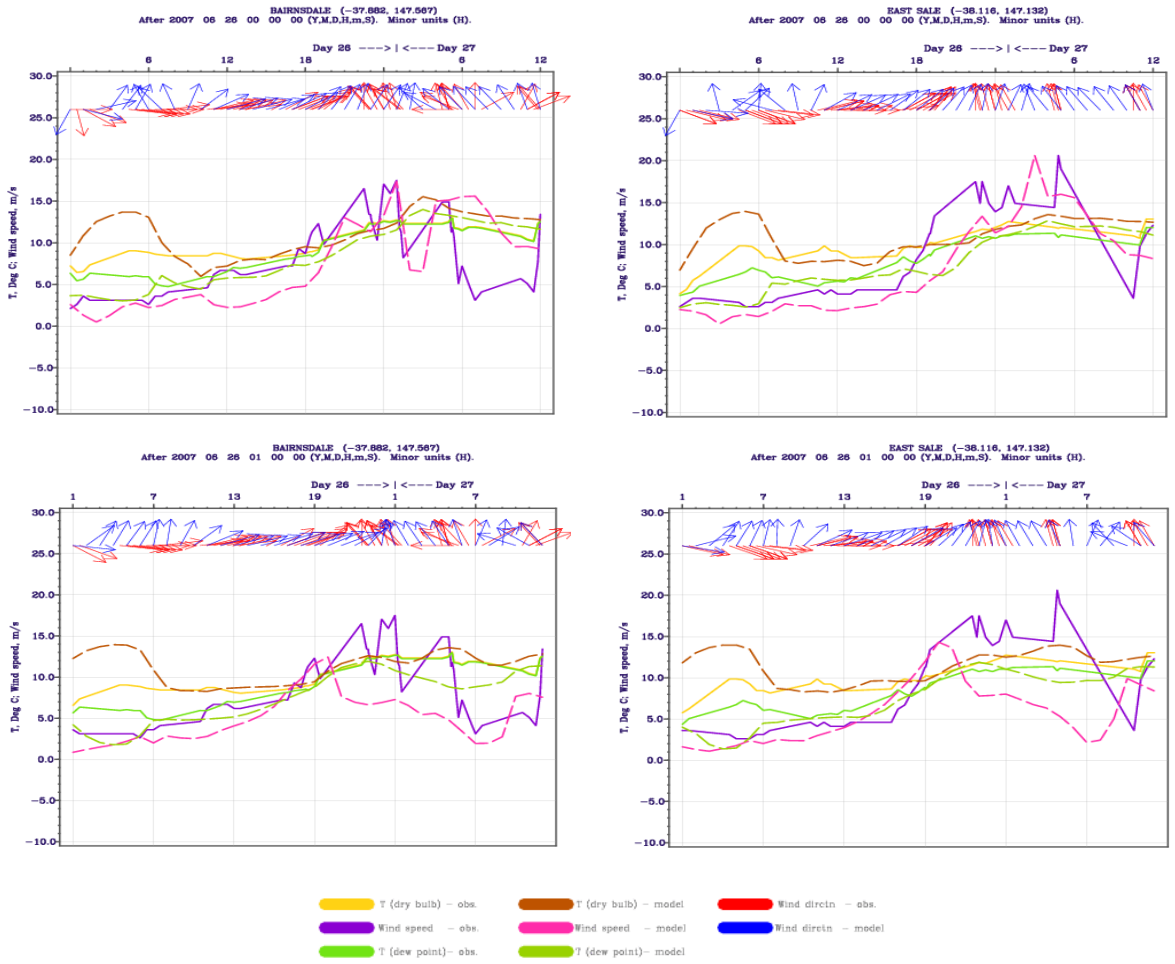

Figure 8. *Time series for 10m wind speed, direction, dry air temperature and wet bulb temperature for MALAPS (top) and MesoLAPS (bottom) compared against observation for Bairnsdale (right) and East Sale (left). Observations (solid) and Model (dashed).*

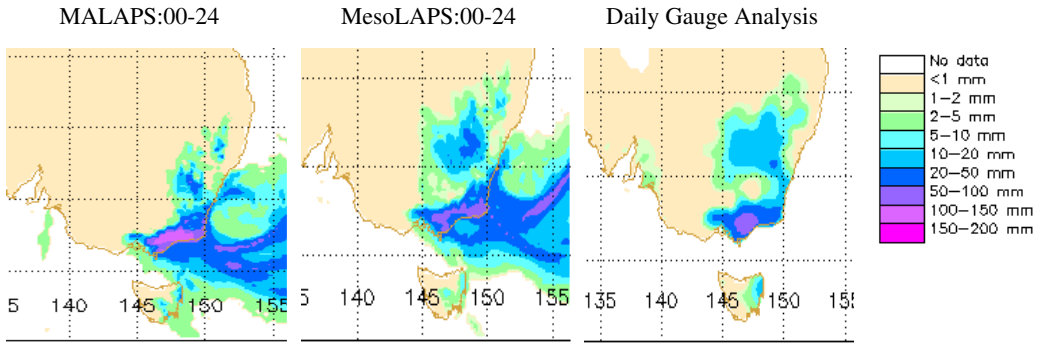

Figure 9. *24 hour Rainval analysis for MALAPS (left), MESOLAPS (centre) and Analysis (right) up until 27th June 2007 at 00z. All analyses are done at 0.25° keeping the analysis grid uniform for all the systems.*

In addition to the above assessments, RAINVAL package (Ebert and McBride, 1997) was used to test the models' ability to forecast rain 24 hours ahead in time (see Figure 9). It can be clearly seen that both MALAPS and MesoLAPS were able to predict the heavy rainfall in the Gippsland area. It can also be seen that the region of rainfall between 5-10 mm in the southern New South Wales was not captured very well by MALAPS, however MesoLAPS has successfully predicted that feature. Also, MALAPS rainfall intensity is somewhat higher than observed, while the MesoLAPS forecast is more successful. It should be mentioned here that the rainfall forecast for both NWP systems is compared against a coarser-scale analysis.

Discussion and Conclusions

It is important to assess model performance independently during the rare, but severe events that can cause catastrophic damage to infrastructure, since the performance during such events will be largely obscured in area-averaged monthly statistics. Traditionally, numerical weather prediction models have been able to provide only limited guidance in these events, and while the MALAPS forecasts are not perfect, the improvements that we see are very promising.

It can readily be seen from the time series plots that even a forecast that is very good with its forecast of the position of the low pressure system can end up with major errors in the actual wind forecast at critical point locations due to very small errors in position or structure (Vincent *et al.*, 2007). In the case of the 20070626 east coast low, the MALAPS error in the position of landfall was of the order of 1 degree, or 10 gridpoints – a large enough error to cause the dramatically incorrect wind forecast at Mallacoota. However, MALAPS provided very good forecast guidance for areas further to the west. It can be concluded from the results that using an assimilation system and better nesting fields have improved the initial conditions of MALAPS and has thus produced better forecast than MesoLAPS for this case.

References

Ebert, E.E. and J.L. McBride, 1997, Methods for verifying quantitative precipitation forecasts: Application to the BMRC LAPS model 24-hour precipitation forecasts, BMRC Techniques Development Report No. 2, Bureau of Meteorology Research Centre, Melbourne, 87 pp.

Harris, B., C. Tingwell, P. Steinle, W. Bourke, M. Naughton, G. Roff and J. Paevere, 25-31 May 2005, Use of Level-1D radiances in GASP, Bureau of Meteorology Research Centre, International ATOVS Working Group, Beijing, China

Steinle, P.J, 18-22 April, 2005: Generalized Statistical Interpolation, Proceedings of the 4th World Meteorological Organisation Symposium on Assimilation of Observations for Meteorology and Oceanography, Prague, Czech Republic.

Tingwell, C., B. Harris, P. Steinle, W. Bourke, M. Naughton, G. Roff and J. Paevere, May 2005, Assimilation of Level-1D ATOVS Radiances in the Australian Region LAPS System, Bureau of Meteorology Research Centre, International ATOVS Working Group, 25-31, Beijing, China.

Vincent, C.L, W.P. Bourke, J.D. Kepert, M. Chattopadhay, Y. Ma, P.J. Steinle and C.I.W. Tingwell, Verification of a High-Resolution Mesoscale NWP System, In Press, Aust. Meteor. Mag, 2008.